Development of a Laser-Guided Variable-Rate Sprayer with Improved Canopy Estimations for Greenhouse Spray Applications

Thesis

Presented in Partial Fulfillment of the Requirements for the Degree Master of Science in the Graduate School of The Ohio State University

By

Uchit Nair

Graduate Program in Food, Agricultural & Biological Engineering

The Ohio State University

2020

Thesis Committee

Dr. Peter Ling

Dr. Heping Zhu

Dr. Ajay Shah

Abstract

Traditional greenhouse spray technologies are wasteful, with large off-target losses. These chemicals when used in such excessive quantities can be harmful to the environment and create a hazardous work environment for greenhouse workers. The efficiency of the spray system can be improved by using an intelligent variable-rate sprayer. It was able to achieve a reduction in spray volumes by about 45% even with a limited accuracy in its characterization of plant canopies (Yan et al., 2018). The efficiency of the variable-rate system can be improved further by improving its characterization of plant canopies. This was achieved by processing the data obtained from the laser sensor. The processing algorithm (CHBC) developed was a combination of a registration algorithm, clustering algorithm and mirroring. The registration algorithm was used to improve resolution. The clustering algorithm segmented individual plant canopies from the laser data to enable further processing of each canopy separately. Mirroring was used to predict the occluded portions of the plant canopies. CHBC was shown to reduce root mean square error (RMSE) in the canopy width measurements by 46%. It achieved an overall mean RMSE of 25 mm compared to 47 mm recorded by Yan et al. (2018). The sensor height was indirectly proportional to the RMSE recorded by CHBC up to a certain height, after which the RMSE stayed the same. The 'optimal' sensor height for the best performance was calculated based on the limitations of CHBC. The CHBC algorithm was integrated into an existing real-time/inline system developed by Yan et al. (2019) with modifications. The inline operation was converted to an offline operation. A new GUI was designed, and the modifications made to the system were tested in a lab environment to ensure proper function. A convex hull algorithm was also introduced to measure volumes and consequent spray rates for the offline system. The convex hull method was more accurate in measuring volumes, achieving a mean accuracy of

81% compared to 66% when using the Yan et al. (2019) methodology. This improved volume estimation accuracy also resulted in spray savings of 15%. The performance of the offline system was tested in a greenhouse environment by measuring the spray coverage achieved over plant canopies. The offline system managed to significantly reduce spray coverage at the edges of the plant while still maintaining recommended deposition. The coverage at the tops and bottoms of plant canopies with tight row spacing was similar for all systems. The offline system significantly reduced coverage below recommended values at the bottom of canopies with large row spacing. The spray density for these canopies was still sufficient for disease prevention using insecticides and herbicides but not for fungicides. The offline system achieved spray savings of 87% compared to the conventional spray system while also improving the efficiency of the Yan et al. (2019) system by 53%.

Acknowledgements

I will be forever indebted to Dr. Peter Ling for his support, guidance, and mentorship throughout the two years that I have been at Ohio State. He has consistently brought out the best in me and challenged me to be better. I am extremely grateful for him giving me the opportunity to pursue a master's degree at Ohio State and helping me every step of the way.

I thank Dr. Heping Zhu for always giving me his time, guidance, and his willingness to patiently explain in detail any concept that I was struggling with. I thank Dr. Ajay Shah for helping me settle in at Wooster when I first arrived and for his guidance through these two years.

I thank Adam Clark for being so enterprising and helping me setup experiments like they were his own. I am grateful for all his suggestions, advice and for his patience during all the long days spent at the greenhouse.

I sincerely thank Candy McBride for working so hard on my fellowship justification. I would not be at Ohio State if not for her. I thank Peggy, Mary, and all the staff at FABE in Wooster for their continues support throughout my time there.

I thank Andrea Landaverde, Aditya Raj, Luis Huezo, Asmita Khanal, Kaylee South, Parisa Nazemi, Ramon Salcedo, Shyam Sivaprasad, Anirudh Akula, Jhony Mera, and Anton Walter for making Wooster feel like home and giving me memories that I will cherish for the rest of my life. I could not have imagined a better group of people to have spent the last two years with.

Vita

2014–2018 ……B.Tech Electrical and Electronics Engineering, Sri Ramaswamy Memorial Institute of Science and Technology

2018-Present…. MSc. Food, Agricultural and Biological Engineering, The Ohio State University

Field of Study

Major Field: Agricultural Engineering

Table of Contents

List of Tables

List of Figures

List of Equations

Chapter 1: Introduction

1.1 Background

Greenhouse production systems provide a highly controlled environment that allows for plants to flourish. It achieves this control by mitigating the effects of the surrounding environment and therefore, removing variability. However, these control measures come at a cost. They are very expensive to run and therefore need to have all systems running at a high efficiency in order to make economic sense. However, existing greenhouse spraying systems used are wasteful and inefficient. Greenhouse growers believe that a high spray volume and pressure is needed for good plant protection (Braekman et al., 2009; Goossens et al., 2004). This is a wasteful and unsafe practice since the chemicals used are highly toxic and can have lasting effects on the environment and human health.

Runoff from greenhouses may exceed environmental risk limits and chemical concentrations have been found to exceed those from agricultural runoff (Roseth and Haarstad, 2010). High concentrations of chemicals with high water solubility was found in water bodies and groundwater near greenhouses as well as in the products grown inside them (Haarstad et al., 2012). The excessive use of chemicals inside greenhouses creates a hazardous work environment. Greenhouses are closed off when compared to an open field and this can lead to the chemicals staying inside the greenhouse for much longer times, resulting in prolonged exposure for workers (Siebers and Mattusch, 1996; Tsimbiri et al., 2015).

These chemicals are known to be carcinogenic, cause cardiovascular abnormalities, as well as neurological symptoms such as Parkinson’s disease (Cayir et al., 2019; Çayir et al., 2018; Del Prado-Lu, 2007; Semchuk et al., 1992). Therefore, it is vital to use these chemicals as sparingly as possible but still manage to get the best properties out of them - the easy control or prevention of plant pathogens, pests, weeds and diseases. Damalas and Eleftherohorinos (2011) suggest various ways of reducing the use of chemicals such as implementing less pesticide dependent cropping systems, the development of new chemicals that are safer and using the right spray system. An improved spray system can significantly improve the efficiency of pesticide use and can reduce spray volumes.

Conventional, fixed-rate spray technology has large off-target losses and poor deposition (Giles et al., 2011; Pergher et al., 1997; Sánchez-Hermosilla et al., 2011; Seiber et al., 1993). Spray volume can be reduced significantly by using variable-rate spray technology. This has been well documented for field applications. The principle of the variable rate sprayer is to obtain a visual of the canopies to be sprayed and control the spray rate of the nozzles based on the characteristics of the canopies. The visual can be obtained using a camera, ultrasonic sensor or laser sensor. Cameras have a limited field-of-view, provide only 2D data and their performance is affected by environmental factors such as lighting conditions (Giles et al., 2011). Ultrasonic sensors have a limited spatial resolution and their performance is also affected by environmental variables (Chen et al., 2012). A laser sensor is best suited for this operation and has been documented to perform well under field conditions (Jeon and Zhu, 2012; Shen et al., 2017; Chen et al., 2012; Zhu et al., 2017). Chen et al. (2012) developed a laser sensor guided, variable rate spray system for field applications. The laser sensor was used to calculate the volume and density of canopies which then determined the amount of spray volume required. The spray rate was controlled by using PWM controlled nozzles which were triggered in real time as the laser sensor passed over a target canopy. The reduction in chemical use was between 47 and 73%.

Shen et al. (2017) provided a similar improvement by using the same principle and observed an improvement in the coverage while using a significantly lesser volume of chemical. They found that in the variable rate mode the sprayer used only 12.1 to 43.3% of the chemical used in the constant or fixed rate mode. The coverage also improved by 30 to 55%. Giles et al. (2011) evaluated the performance of different target-sensing, smart sprayers in three orchards with varying row spacing and tree species. They observed that the savings in spray volumes was proportional to gaps between tree rows since the most tightly packed orchards showed 15% spray savings whereas the orchards that had wider tree row spacings showed a reduction of 40% in the spray volume used.

The same principle of using a laser-guided, variable rate sprayer can be applied inside greenhouses but it requires modifications. Row spacing is very limited inside greenhouses since greenhouse productions systems are expensive to run and hence growers need to maximize the yield per square foot. Hence, to improve spray efficiencies for tight row spacing and small gaps, the accuracy of canopy volume and density measurements must be high (Giles et al., 2011). The resolution of the 3D map generated by the laser sensor will need to be higher since the target objects are a lot smaller and are more tightly packed.

There is limited literature regarding the use of a smart, target-sensing, variable-rate sprayer inside greenhouses. Satnam Singh et al. (2004) designed an autonomous vehicle for greenhouse spraying with the objective of improving worker safety inside greenhouses but not to improve spray efficiencies. Sánchez-Hermosilla et al. (2013) studied the effects of controlling the spray volume application rate based on a manually calculated Plant Row Volume (PRV) rather than a laser sensor based system. Llop et al. (2016) studied the accuracy of using a 2D laser sensor to characterize tomato plants inside greenhouses. The tomato plants were mapped from both sides to determine their height, volumes, width, and leaf area. This system, though accurate, was built for mapping high-wired tomato crops and not short crops grown in greenhouses which have a very different canopy geometry.

Yan et al. (2019) studied the performance of an intelligent, 2D laser sensor guided, variable rate sprayer for greenhouse applications. They used a system to map plant canopies from above, enabling the characterization of short crops. They observed spray savings of about 45%. However, the accuracy of the 2D laser sensor in determining dimensions of 3D objects was limited (Yan et al., 2018). The RMSE (Root Mean Square Error) in the width measurements increased as the horizontal distance of the object from the laser increased. The point cloud data was heavily distorted and more and more of the target objects were hidden from the laser sensor as the distance of the targets from the laser increased. This system can therefore be improved further by overcoming the shortcomings in canopy characterization.

This project focuses on improving and modifying the Yan et al. (2018) and Yan et al. (2019) system by introducing a processing algorithm to improve plant canopy characterization. The processing algorithm will need to manipulate the data obtained from a laser sensor and make more accurate estimations of the plant canopy volumes and densities – the factors that determine the spray volume output. The improved canopy characterization algorithm is incorporated into the Yan et al. (2019) system by converting the inline operation of the system to an offline operation. The performance of the modified system is tested in a lab environment as well as in the greenhouse.

1.2 Objectives

The overall objective of this project is to improve the spray efficiency of a 2-D laser guided, variable-rate sprayer for greenhouse applications by making more accurate canopy volume and density estimations.

The specific objectives are:

- To implement a processing algorithm that can characterize plant canopies more accurately.
- To test the variables that affect the performance of the processing algorithm.
- To redesign the existing inline Yan et al. (2019) system to integrate the processing algorithm.
- To conduct lab and field experiments to evaluate the performance of the modified variable-rate spray system.

1.3 Thesis Organization

This thesis is organized into four chapters. The first chapter is an introduction and provides a brief background of the study, the problems being addressed, as well as the goals and objectives of the rest of the study. The next two chapters will be presented in the form of two standalone manuscripts. The first of the two manuscripts (Chapter 2) will address the development of the processing algorithm used and its performance. It will describe in detail the methodology used to improve canopy characterization as well as provide comparative results with the existing methodology. The physical limitations-such as sensor height, to the performance of the algorithm are also discussed. The second manuscript (Chapter 3) will discuss the methods used to integrate the processing algorithm developed in the previous chapter into an existing variable-rate spray system and test its performance in the lab as well as in a greenhouse. It will discuss all the modifications necessary and introduce an improved method to determine plant canopy volumes and spray rates. The final chapter (Chapter 4) will be an overall conclusion of the thesis with recommendations on future studies and further improvements that can be made to the system.

Chapter 2: Improved Canopy Characterization with Laser Scanning Sensor for Greenhouse Spray Applications

2.1 ABSTRACT

Laser-guided intelligent spray technology for greenhouse applications requires sensors that can accurately measure plant dimensions. This study proposed a new method to overcome current limitations by introducing a processing algorithm that manipulates the noisy dataset and determines the optimal sensor height to produce better measurement of the canopy width. The processing involves a combination of registration, clustering and mirroring algorithms. The registration algorithm aligns multiple scans of the same scene to improve resolution. The clustering algorithm isolates individual plant canopies from the dataset to enable further processing. The mirroring algorithm resolves the problems of distortion and occlusion and predict the missing information in the dataset. The performance of the processing algorithm was evaluated by calculating the root mean square error (RMSE) in the canopy width measurements. Its results were compared with the measurements reported in Yan et al. (2018). The processing algorithm reduced RMSE values by 46% compared to Yan et al. (2018). The average RMSE of the processing algorithm was 25 mm compared to 47 mm by Yan et al. (2018) when the laser sensor was at a height of 1 m. The sensor height was observed to be inversely proportional to the RMSE values. Another experimental setup was used to test the limits of this relationship while using objects that were more representative of plant canopy shapes. The accuracy of the CHBC algorithm reduced when the sensor height was either above or below the ‘optimal sensor height’ which was derived from calculations made by Sun et al. (2017). The processing algorithm introduced has the potential to not only improve spray efficiencies but also in plant phenotyping applications.

Keywords: Automation, Clustering, LiDAR, Point Cloud Data Processing, Variable-Rate Spray

2.2 INTRODUCTION

Chemicals are used in greenhouses to maintain plant yield, and quality by combating insects, weeds, and plant pathogens, but they may be used in excessive quantities by greenhouse growers (Braekman et al., 2009; Goossens et al., 2004). This excessive use can have a detrimental effect on the environment as well as on worker safety. Runoff from greenhouses may have levels of pesticides, - including fungicides, herbicides and insecticides that are hazardous (Haarstad et al., 2012; Roseth and Haarstad, 2010). Excess chemicals from commonly used spray systems such as handheld sprayers and fixed-rate spray booms (Derksen et al., 2008; 2010) stays in the greenhouse and compromises worker health (Siebers and Mattusch, 1996). Chemical exposure has been shown to cause health issues for greenhouse workers (Cayir et al., 2019; Çayir et al., 2018; Damalas and Eleftherohorinos, 2011; Del Prado-Lu, 2007). Pesticide residues on greenhouse crops also present a food safety concern (Osman et al., 2011). Therefore, there is a need to improve the efficiency of chemical use in greenhouses by reducing both the volume of chemicals and the drift from spray systems.

Laser-guided variable-rate sprayers have shown a significant improvement in spray efficiency for field applications (Berenstein et al., 2010; Gil et al., 2007; Giles et al., 2011; Jeon and Zhu, 2012; Shen et al., 2017; Chen et al., 2012; Chen et al., 2013). The spray volume is controlled based on measured plant canopy characteristics. These measurements can be carried out by using cameras, ultrasonic sensors, or LiDAR/laser sensors. The performance of camera image based canopy characterization is dependent on the lighting conditions (Llorens et al., 2011) and only provide 2D data which has a limited field of view. Ultrasonic sensors can provide 3D data but their performance also depends on environmental conditions (Chen et al., 2012) and their detection accuracy is much lower than laser sensors (Llorens et al., 2011). Laser sensor based canopy characterization has been demonstrated in the field to be a very effective tool in not only determining spray volumes but also in informing management practices (Chakraborty et al., 2019; Escolà et al., 2017; Llorens et al., 2011). It can be used for fruit detection and yield prediction (Gené-Mola et al., 2020; Méndez et al., 2019). It has potential in plant phenotyping (Colaço et al., 2018; Heun et al., 2019; Sun et al., 2017; Wang et al., 2017), disease detection (Husin et al., 2020), making accurate measurements of leaf morphological traits, leaf area index, as well as leaf area density (Llop et al., 2016; Panjvani et al., 2019; Thapa et al., 2018).

Compared to orchards, canopy characterization inside a greenhouse can be challenging due to multiple constraints that must be addressed. Greenhouse production is expensive; therefore, high-value plants are tightly packed and require precise care and attention. The resolution, therefore, of the mapped data needs to be high due to the dense grouping of plants as well as the smaller targets compared to orchards. The laser sensor must be placed above the canopy to maximize the number of rows of plants that can be mapped from one scan. In an orchard, the sensor is placed at a height of 1.5 to 2.0 m above the ground and travels between rows (Escolà et al., 2017; Gené-Mola et al., 2020; Gil et al., 2007; Liu and Zhu, 2016; Llorens et al., 2011), mapping the side-view of trees that are about 4.0 m tall and hence the area to be mapped is about 2 m either side of the laser sensor. In a greenhouse on the other hand, the length of a bay is much greater than 2 m so the area to be mapped either side of the overhead laser sensor must be large. This prevents certain portions of the plant canopies out of the line-of-sight of the laser sensor, a condition referred to as occlusion. The resolution of the laser sensor also decreases as the horizontal distance from the sensor increases (Sun et al., 2017). To reduce the effects of occlusion, the sensor can be placed higher, but this also reduces the resolution (Sun et al., 2017).

Researchers have characterized tomato canopies inside greenhouses using a similar approach reported for orchard and nursery applications. The tomato plants were grown on high-wires and side-views were scanned (Llop et al., 2016). However, this methodology is not suitable for short crops such as potted plants where plant canopy information is better collected from an overhead view. Yan et al. (2018) studied a laser sensor mounted on a horizontal spray boom system that scanned the targets from above, but it suffered from occlusion and resolution problems. These problems resulted in difficulties in making accurate canopy width measurements and distinguishing between individual plant canopies that were farther from the laser. The dataset became sparser and more distorted as the distance from the laser sensor increased. These limitations can be addressed by either a hardware solution, e.g. use more laser sensors to collect more data, or a data processing algorithm to extract more reliable information from the data set.

The use of multiple laser sensors can reduce occlusion and provide more canopy structure information. Heun et al. (2019) used two sensors to map plant canopies from above. Gené-Mola et al. (2020) found that by combining data from multiple laser sensor placed between rows at different heights, the accuracy of the system was improved. However, the range mapped by the dual laser systems used was only about 3.5 m (Gené-Mola et al., 2020; Heun et al., 2019). Mapping the whole field with this limited range is time consuming but possible in a field setting where the system can travel between tree rows, which is not possible in greenhouses. To map a large greenhouse bay and maintain a high resolution, it would require multiple sensors which is not feasible because it significantly increases the system cost.

The resolution of the system can be improved in other ways such as ‘super resolution’ algorithms or by implementing ‘registration’ algorithms. Super-resolution can be performed by either using a single image or combining multiple scans. Single scan super-resolution requires a training dataset with multiple images which is highly time-consuming to obtain (Glasner et al., 2009; Hornacek et al., 2013; Mac Aodha et al., 2012). Multi-scan super-resolution requires at least 30 scans in order to show a significant improvement in resolution (Bulyshev et al., 2014; Kil et al., 2006). The large number of scans is not feasible for greenhouse applications mainly because it is a time-consuming process to scan the large growing areas. Our main objective was to improve estimations of plant canopy width measurements, not resolution. A marginal improvement in resolution that could assist the clustering algorithm in grouping datapoints more accurately was sufficient. Therefore, ‘registration’ can be used in this context. Registration is the process of aligning multiple scans of either the same scene or multiple angles of the same scene where each scan has some overlapping area with the previous scan (Besl and McKay, 1992; Guo et al., 2014; Mitra et al., 2004). Scans from multiple angles can reduce the area that is occluded but requires multiple laser sensors, which increases the cost of the system significantly. Because the registration algorithm is only used to assist the performance of the clustering algorithm, a simple, rudimentary form of the Iterative Closest Point (ICP) principle has been shown to be sufficient (Besl and McKay, 1992).

To predict the occluded portions of each plant canopy, information from the parts of the canopy visible to the laser sensor can be used. This requires each canopy to be processed individually. A clustering algorithm can isolate individual plant canopies from the laser sensor dataset. Clustering is the grouping of data such that points within a cluster are more ‘similar’ to each other than the rest of the point cloud. In a spatial dataset, ‘similarity’ can be defined through Euclidean distance. Points that are closer together are assumed to be more ‘similar’ to each other than those further apart. Any points that lie below a certain threshold value of Euclidean distance are considered as part of the same cluster. The threshold values are set by the user and they can be fixed, dynamic or used in combination with other parameters. There are multiple variations of clustering algorithms that can be used for varied applications. The dataset in this project was noisy and distorted and hence algorithms whose performance is sensitive to threshold values set by user-defined parameters (Bosnak, 2017; Ester et al., 1996; Ghosh and Lohani, 2013; Jain et al., 1999; Nyström Johansson and Wellenstam, 2017; Reiser et al., 2018; Wei et al., 2014) would not be expected to perform well. Clustering algorithms that are based on training models (Spinello and Siegwart, 2008; Wang et al., 2008) cannot work for this dataset either because only a portion of plant canopies is visible to the laser and there is significant distortion. Therefore, it becomes unreliable to make comparisons to pre-defined plant canopy profiles. Hence, the clustering algorithm used for this application was less sensitive to user-defined threshold values and did not require training models.

Processing algorithms, however, have some limitations in performance depending on the quality of data received. The quality of the dataset was restricted by some physical limitations such as the height at which the laser sensor was placed. Yan et al. (2018) found that the height of the laser sensor determines how much of the plant canopy is hidden. The height of the sensor is also inversely proportional to the resolution of the dataset (Sun et al., 2017), resulting in the laser sensor potentially missing the edges of plant canopies. The optimal height of the laser sensor must therefore be determined to ensure the best performance of the processing algorithm.

Specific objectives of this research included –

- Develop a processing algorithm that isolates plant canopies from the dataset.
- Compare the processed dataset's width measurement accuracy to Yan et al. (2018).
- Test the effect of sensor height on the accuracy of canopy width measurements.

2.3 MATERIALS AND METHODS

2.3.1 Data Collection

There were two data sets for this project. The first of which was obtained from Yan et al. (2018). The LiDAR/laser sensor scans were taken under indoor conditions at the USDA-ARS Application Technology Research Unit in Wooster, Ohio. The test area was 5.0 m wide, 8.0 m long and 5.5 m high. The laser sensor was mounted on the left side of a linear constant-speed track, which moved the laser over 4 rows of regularly shaped objects and one row of artificial plants. Each row consisted of the same object and in the case of the artificial plants, similar shape and volume. Images of these regularly shaped objects and artificial plants are given in Yan et al. (2018). The four regularly shaped objects were a toy ball, a cardboard box, a basketball and a cylinder (Table 2-1). These objects were chosen to provide a clear standard against which the performance of the algorithm could be compared. The toy ball was pink and had a smooth surface, the basketball had an alternating pattern of red and black with a textured finish, the box was made of cardboard and the cylinder was white, with a smooth finish. Artificial plants were used as their foliage volumes and shape remain constant during the experiment. The objects were placed on wooden boards of variable height to keep the distance from the top of every object to the laser sensor uniform, irrespective of the dimensions of each object. Each row had 8 of the same objects placed 0.5 m apart with the first object placed directly underneath the sensor travel path, with the eighth object at 3.5 m horizontally from the laser sensor. For comparisons in this paper, the data was calculated for 5 different laser sensor heights (distance from the top of the objects to the laser). The laser sensor height started at 0.25 m and increased in increments of 0.25 m. Its travel speed was 1.6 km/h. Each scan was iterated 3 times.

Table 2-1: Dimensions of objects used in the dataset collected by Yan et al. (2018). Standard deviations are given within parenthesis.

Target Object	**X (Width) (mm)**	**Y (Length) (mm)**	**Z (Height) (mm)**	**Diameter (mm)**
Artificial Plants	231 (20)	232 (22)	325 (8)	
Basketball				183
Box	231	225	115	
Toy Ball				233
Cylinder			108	118

A second dataset was collected to evaluate the effect of sensor height on the plant canopy characterization. The experimental setup was similar to the first dataset described above. The only differences were the travel speed, the mounting height of the sensor and the target objects. The sensor travel speed was 0.48 km (0.3 miles) per hour. The laser sensor was mounted at 5 different heights – 2.00, 2.25, 2.50, 2.75 and 3.00 m from the ground. The objects used were 3 rows of artificial plants (Plant Group-1,2,3) and 1 row of 'Regular Objects' which were toy balls placed over pots that emulated an "ice-cream cone" shape (Table 2-2, Figure 2-1). These objects were used to better represent plant canopy shapes in a greenhouse. The artificial plants within rows had similar dimensions but the dimensions varied between rows. Seven objects were placed in each row, 0.5 m apart, starting from 0.5 m from the laser up to 3.5 m. The spacing between rows was also 0.5 m.

Table 2-2: Dimensions of target objects used to test the effect of sensor height. Standard deviations are in parenthesis.

Object	X (Width) (mm)	Y (Length) (mm)	Z (Height) (mm)	Diameter (mm)
Plant Group-1	231 (20)	232 (22)	325 (8)	
Plant Group-2	184 (14)	173 (16)	205 (12)	
Plant Group-3	239 (9)	206 (21)	331 (10)	
Regular Object			345	233

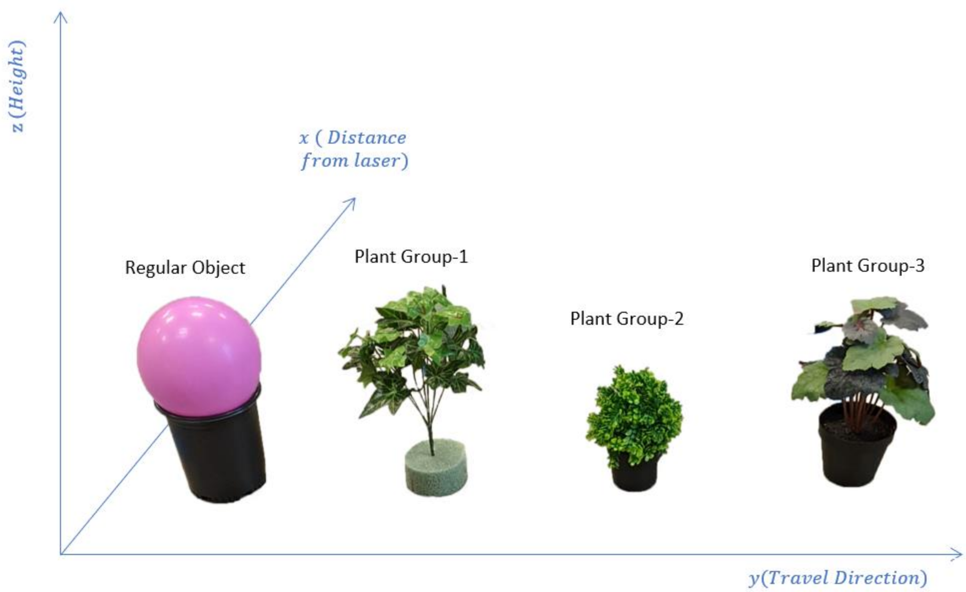

Figure 2-1: Target objects used for the second dataset to test the accuracy of canopy dimension measurement using the processing algorithm. Three sets of irregular shaped objects and one set of regular shaped objects were used.

2.3.2 Laser sensor and 3D map construction

The information obtained from the laser sensor was converted to a three-dimensional map/ point cloud dataset. The laser sensor used was a 2D laser sensor with a 10.0 m, 270˚ radial range with 1080 laser beams per scan cycle of 25 ms (UST 10-LX, Hokuyo, Osaka, Japan). The sensor works based on the time of flight principle. It sends out a laser beam of a known speed and measures the amount of time the beam takes to reflect from an object or surface and return to the sensor to determine the range data (‘r’). Each beam from the sensor is rotated from the previous one by 0.2˚, starting from -135˚ up to 135˚. This provides a total radial scanning range of 270˚. Hence, each laser beam has a corresponding scanning angle ‘Ɵ’ as well as range data ‘r’. The ‘height’ (Z-axis) and ‘width’ (or ‘Distance from the laser sensor’) (X-axis) of each laser beam can be determined by using Equation 2.1 and Equation 2.2, derived from the Pythagorean theorem. The third dimension- ‘length’ (Y-axis), is obtained by moving the sensor through space via the constant speed track as shown in Figure 2-2.

$$X = r \times sin\theta \quad (2.1)$$

$$Z = r \times cos\theta \quad (2.2)$$

Where, ‘X’ is the horizontal distance from the laser sensor to the detection point on the canopy (m)

‘Z’ is the laser sensor height above the top of canopy (m)

‘r’ is the range data from the laser sensor

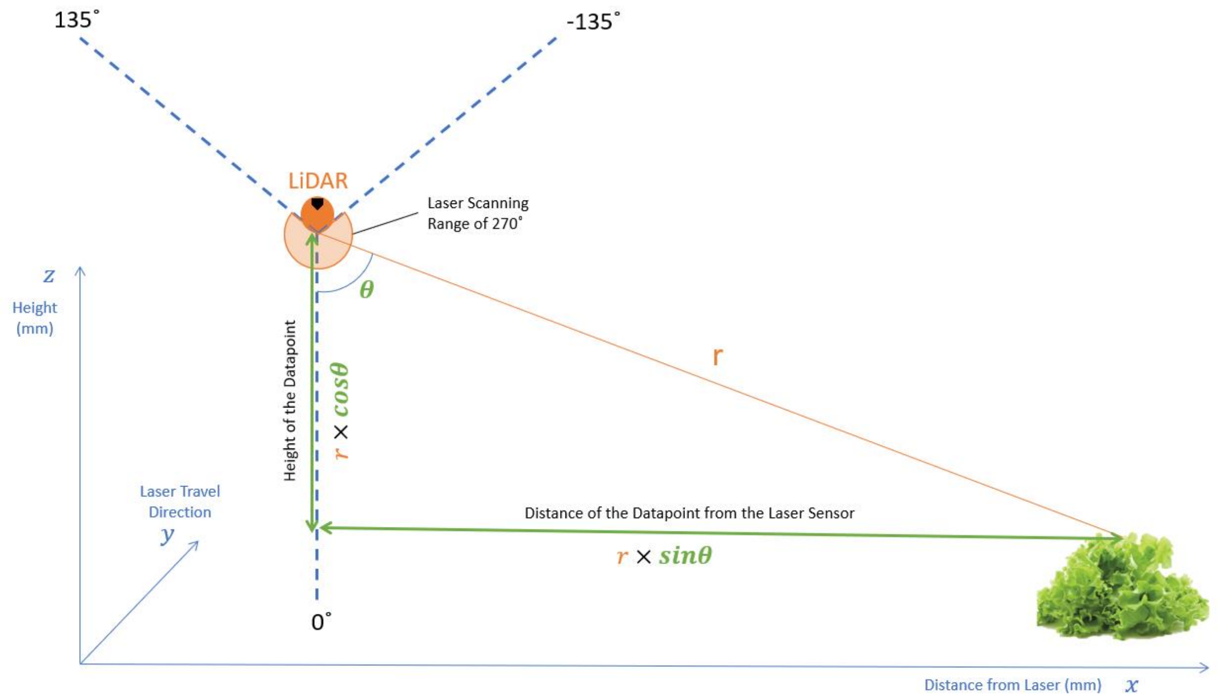

Figure 2-2: Construction of the point cloud dataset. The laser sensor scans along X-axis and travels along Y-axis. The height and distance of each point from the laser is calculated by using its respective scanning angle 'Θ', the distance travelled before.

The constant speed of the laser sensor was used to calculate the Y-coordinates and provide a complete three-dimensional map/point cloud. The sensor produced 1080 beams every 25 ms (time taken for one scanning cycle), or one beam every 0.0231 ms (25 ms/1080). The distance that each laser beam was deviated from the previous beam in the Y direction (Laser travel direction) was therefore given by Equation 2.3.

$$Y = 0.0231 \times v \tag{2.3}$$

Where, 'Y' is the distance that the laser beam travelled (mm)

'v' is the laser sensor travel speed (m/s)

The resulting 3D point cloud was visualized and processed entirely on a numerical computing platform (MATLAB R2019a ver. 9.6.0.1114505, MathWorks, Natick, Massachusetts, USA). The data was then filtered to get rid of the datapoints that represent the ground/greenhouse floor because they interfere with the clustering algorithm. They were removed by manually measuring the height of the sensor from the ground and removing any points below that threshold. The remaining points represent the plant canopies or objects. One half of the dataset was also removed because only one half of the 270˚ scanning plane had objects as they were only placed to the right of the sensor and nothing was placed to the left.

2.3.3 Processing methodology

The data was processed to identify individual objects and improve canopy width measurements. The processing algorithm involved registration, clustering, and mirroring. To improve the resolution of the dataset, registration was used. A clustering algorithm was used to extract individual targets from the data set for further processing which included mirroring each target to get a better estimate of its shape and dimensions.

2.3.3.1 Registration

A rudimentary point-to-point Iterative Closest Point (ICP) Registration was performed to align multiple scans of the same scene (Besl and McKay, 1992). The basic principle of this algorithm is to find the best transformation that must be performed on one point cloud so that it is aligned with the reference point cloud. This requires a two-step process of data association and transformation. Data association is essentially finding point-pairs between the two point clouds. Every point in the reference point cloud is associated/paired to the point that is closest to it in the second point cloud. The transformation matrix is then determined such that the distances between these point pairs is minimized. This involves finding the center of mass of the two point clouds, translating the second point cloud onto the reference point cloud, and finding the rotation required through singular value decomposition (SVD). This whole process of data association and transformation is then iterated until there is no further improvement in the alignment of the two point clouds. A third scan can then be registered onto the first two scans using the same process. This registration algorithm was implemented using a function developed by Jakob (2020).

Three scans were registered in this project for the purpose of increasing the density of datapoints further from the laser to assist the clustering algorithm. More scans could potentially be registered but each additional scan would require more data collection time and more computation time due to the increase in datapoints.

2.3.3.2 Clustering

To delineate plant canopies from the point cloud data, a clustering algorithm was used. A DBSCAN algorithm groups dense distributions of points in the dataset while being robust to noise (Ester et al., 1996). It works by identifying whether a point is part of the interior of a cluster (core), a border point or just noise based on two user-defined parameters – i.e., a distance threshold and a minimum number of points that must lie within this threshold (density). The DBSCAN algorithm performs well for noisy datasets but it is not robust to clusters of varying densities. This is a significant shortcoming for the dataset in this project because it is known that the clusters (plant canopies) have varying densities as the distance from the laser increases.

To overcome these shortcomings Varied-DBSCAN, a modified DBSCAN algorithm was tested (P. Liu et al., 2007). A dynamic distance threshold was used as opposed to a fixed threshold, that is dependent on the density of the point cloud distribution. A varying distance threshold was determined by using a KNN function that determines the specified number of nearest neighbors from a point and returns their distances. The sum of the mean and 2 standard deviations of these distances were used to determine the distance threshold for that specific point. This was done so that outliers were removed, and under-segmentation did not occur. However, the Varied-DBSCAN algorithm had trouble distinguishing between plant canopies when they were placed closer together (Figure 2-3). When the algorithm was tested inside a greenhouse, it tended to heavily under-segment the dataset.

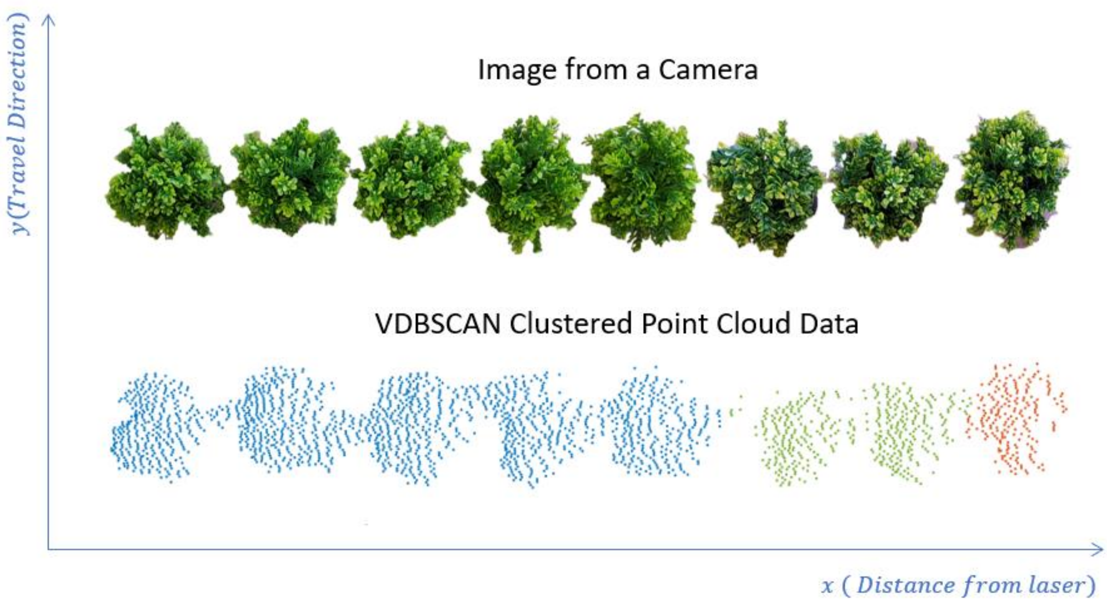

Figure 2-3: Shortcomings of the Varied-DBSCAN algorithm due to under-segmentation when plant canopies are tightly packed. Each color represents an individual cluster. The 3D point cloud was obtained by moving the laser sensor at 0.5 km/h and placing the laser sensor at 0.5 km/h and placing the laser sensor at a height of 2.5 m from the ground.

A clustering algorithm that can effectively isolate canopies even when they are tightly packed is essential for greenhouse applications. Li et al. (2012) developed a clustering algorithm that segmented individual coniferous trees from a dense forest with an accuracy of 86%. They used the wider spacing between trees at their tops to build clusters from the top-down. A clustering algorithm was developed using the same principle. It is fair to assume that for most greenhouse plants, like coniferous trees, the spacing at the tops of the plant canopies are larger than at the bottoms. This algorithm requires a user-defined distance threshold to determine whether two points belong to same cluster or not, but it was not sensitive to this value and was able to group points accurately for a wide range of distance thresholds. For the ease of following discussion, the processing algorithm will be referred to as Canopy Height Based Clustering (CHBC).

CHBC works by grouping datapoints from the top-down, one cluster at a time. All the points are first ordered from the highest to the lowest and clusters are formed one at a time. CHBC assigns each point in the dataset as either 'Part of the cluster' (P) or 'Not part of the cluster' (N). The first step in building a cluster is assigning the highest point (local maxima) in the dataset to 'P'. Each subsequent point is then assigned based on the whether the minimum Euclidean distance between the point in question to any point in the two sets – 'P' and 'N' is lesser than the distance threshold that is set. A distance threshold of half the average row-spacing was found to be a reasonable limit to avoid under or over-segmenting. If the minimum distances to both sets are lesser than the threshold, then the point is assigned to the set that is closer to the point. Therefore, the conditions to be satisfied are:

- If ($Distance\ to\ 'P' <\ Threshold\ \&\ Distance\ to\ 'P' <\ Distance\ to\ 'N'$) then the point belongs to 'P'
- If ($Distance\ to\ 'P' <\ Threshold\ \&\ Distance\ to\ 'P' >\ Distance\ to\ 'N'$) then the point belongs to 'N'
- If ($Distance\ to\ 'P' >\ Threshold$) then the point belongs to 'N'

Once all the points have been assigned to either 'P' or 'N', all the "P" points are grouped as a cluster, stored separately, and removed from the main dataset. The whole process is repeated with all the remaining points. This is iterated until every point in the dataset is assigned to a cluster. This algorithm performed well because it was robust to tight spacing between plant canopies (Figure 2-4) and improved processing times significantly.

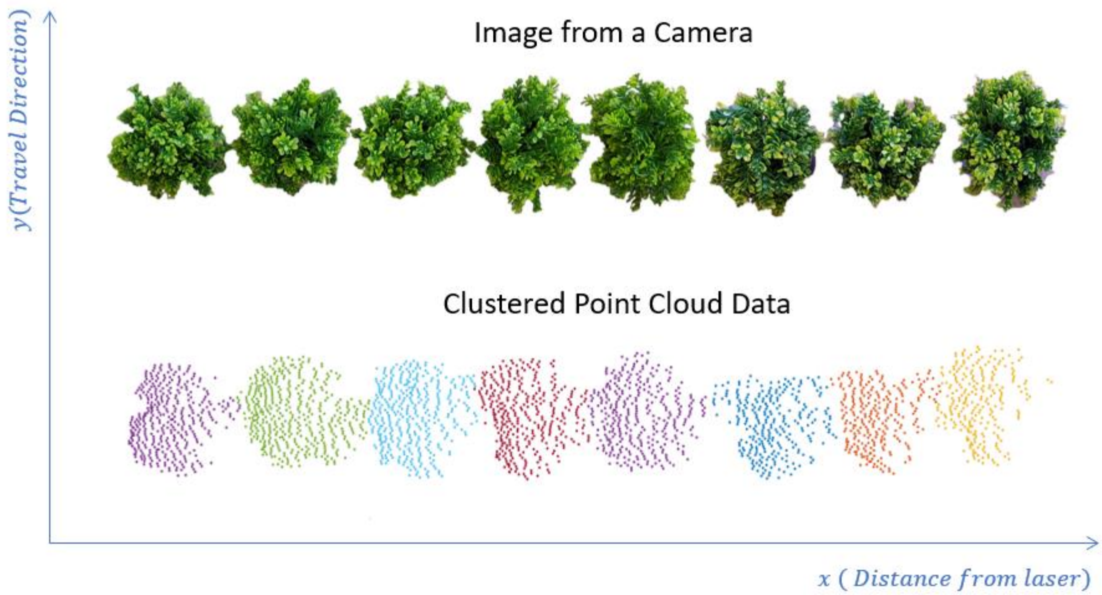

Figure 2-4: CHBC accurately identifies individual plant canopies even when they are tightly packed. Each color represents an individual cluster. The 3D point cloud was obtained by moving the laser sensor at 0.5 km/h and placing the laser sensor at a height of 2.5 m from the ground.

2.3.3.3 Mirroring

As mentioned earlier, only a portion of the canopy is visible to the laser sensor due to the incidence angle and the problem of occlusion. This leads to the large errors in the width measurements made along the X-axis (perpendicular to the laser travel direction). To improve the accuracy of these measurements, a 'mirroring' technique was introduced. It involved assuming that plant canopies are symmetrical and using the visible portion to estimate the dimensions of the whole canopy. This estimate can be achieved by mirroring the front half of the canopy on to the partially occluded rear half side.

The mirroring operation is performed by splitting each cluster down the middle along the Y-axis (Figure 2-5(a)). This is achieved by finding the minimum bounding circle of each cluster (Semechko, 2020). The minimum bounding circle is the smallest circle that contains all points of a given set. This circle is determined for each individual plant by providing each cluster as an input to a function that determines the minimum bounding circle of a given set of points. The diameter of each circle along the Y-axis is used as the axis of mirroring. The points on the front half side are then mirrored across this axis onto the partially occluded rear side. If the objects are to the right of the laser, it means that all the points to the left of the axis are mirrored onto the right and vice versa if the objects are placed to the left of the laser (Figure 2-5(b)). Equations 2.4, 2.5, and 2.6 are used to find the coordinates of the mirrored datapoints. Because each cluster was isolated from the dataset, one can process them individually and perform such operations.

$$X_{mirrored}\ \ (Distance\ from\ laser) = \ -X_{original} + (2 \times a) \tag{2.4}$$

$$Y_{mirrored}\ (\ Travel\ Direction) = Y_{original} \tag{2.5}$$

$$Z_{mirrored}(Height) = Z_{original} \tag{2.6}$$

Where, ‘a’ is derived from x=a which is the equation of the diameter of the circumscribing circle

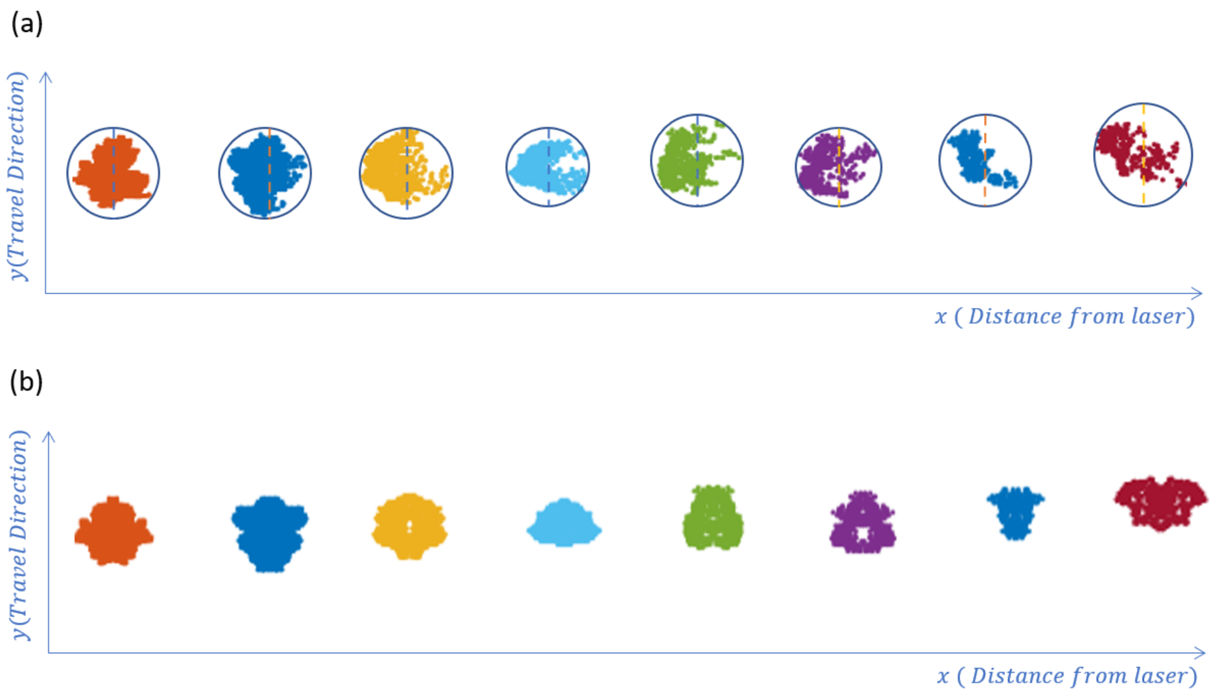

Figure 2-5: Mirroring is a technique used to improve plant canopy estimation. a) The axis of mirroring is the diameter of the minimum bounding circle that is parallel to the y-axis of each cluster. Each color represents an individual cluster. b) The mirrored point cloud data distributions are more representative to plant canopies by eliminating distortion and filling missing points due to occlusion. The datapoints to the left of the mirroring axis are mirrored onto the right. Each color represents an individual cluster.

The dimensions of each individual cluster (target object) was found by measuring the distance between the extreme points along all axes. The relative location of each target object was also found.

2.4 RESULTS AND DISCUSSION

2.4.1 First Dataset Analysis

The CHBC's performance was compared to the measurements obtained by Yan et al. (2018). To facilitate the following discussion, 'width measurement' refers to the measurement taken along the X-axis which is perpendicular to the sensor travel direction. Since the width measurements had the largest error, the Root Mean Square Error (RMSE) in the width was compared to Yan et al. (2018) by utilizing the same dataset. The height of the sensor and the horizontal distance from the laser sensor were the two main limiting factors in the accuracy of measurements by Yan et al. (2018). The effects of these two factors were therefore evaluated and results are shown in Table 2-3 and Table 2-4. The RMSE was measured for 4 sensor heights, 8 horizontal distances from the laser sensor, and 5 target objects.

The sensor height had an inversely proportional relationship with the RMSE in width measurements for all target objects and for both methodologies (Table 2-3). The CHBC algorithm reduced the RMSE at all sensor heights for all objects compared to Yan et al. (2018). The sensor height also had an influence on the RMSE values for CHBC, where the RMSE reduced from 120 mm to 42 mm for the artificial plants, from 100 mm to 13 mm for the toy ball, from 93 mm to 18 mm for the basketball, 106 mm to 34 mm for the box, and from 71 mm to 15 mm for the cylinder. The higher the sensor height, the more of the target that was visible to the sensor and hence the lower RMSE. For the highest sensor height of 1.00 m, the CHBC algorithm reduced the RMSE by 15, 33, 43, 28, 22 mm compared to Yan et al. (2018) for the artificial plants, toy ball, basketball, box, and cylinder, respectively.

Table 2-3: The RMSE of X direction (width) measurements across all horizontal distances of objects from the laser sensor (0.0, 0.5, 1.0, 1.5, 2.0, 2.5, 3.0, 3.5 m) for four sensor heights.

Sensor Height (m)	RMSE in X Direction (mm)			
	Artificial Plants		Toy Ball	
	CHBC	Yan et al. (2018)	CHBC	Yan et al. (2018)
0.25	120	104	100	163
0.50	53	84	30	81
0.75	50	55	12	44
1.00	42	57	13	46
Sensor Height (m)	Basketball		Box	
	CHBC	Yan et al. (2018)	CHBC	Yan et al. (2018)
0.25	93	117	106	132
0.50	36	91	52	78
0.75	25	59	48	48
1.00	18	61	34	62
Sensor Height (m)	Cylinder			
	CHBC	Yan et al. (2018)		
0.25	71	128		
0.50	30	53		
0.75	28	25		
1.00	15	37		

An increasing horizontal distance of the target objects from the laser sensor resulted in an increase in RMSE for both the CHBC algorithm and Yan et al. (2018) (Table 2-4). The CHBC algorithm consistently lowered RMSE compared to Yan et al. (2018) for the objects placed beyond 1.0 m from the laser sensor. There was a steep increase in the RMSE with the CHBC algorithm for the objects placed at 3.0 and 3.5 m from the laser. This was because the CHBC algorithm did not detect the presence of objects for the sensor height of 0.25 m as they were almost completely hidden from the laser sensor. If the data at the sensor height of 0.25 m was not considered, the RMSE would be improved to 55, 18, 55, 48, 39 mm for the objects placed at 3.0 m for the artificial plants, toy ball, basketball, box, and cylinder, respectively. For the objects placed at 3.5 m the RMSE would be improved to 47, 40, 36, 56, 42 mm for the artificial plants, toy ball, basketball, box, and cylinder, respectively.

Table 2-4: The RMSE of X direction (width) measurements across all sensor heights (0.25, 0.50, 0.75, 1.00 m) for eight horizontal distances of objects from the laser sensor.

Horizontal Distance (m)	RMSE in X Direction (mm)			
	Artificial Plants		Toy Ball	
	CHBC	Yan et al. (2018)	CHBC	Yan et al. (2018)
0.0	28	21	14	20
0.5	48	31	15	50
1.0	36	62	16	63
1.5	77	95	21	90
2.0	15	90	4	103
2.5	76	76	37	114
3.0	110	120	71	110
3.5	121	105	121	120
Horizontal Distance (m)	Basketball		Box	
	CHBC	Yan et al. (2018)	CHBC	Yan et al. (2018)
0.0	14	14	58	18
0.5	5	44	21	34
1.0	13	70	30	44
1.5	22	78	39	57
2.0	13	92	29	58
2.5	29	114	66	54
3.0	103	108	123	78
3.5	97	134	91	100
Horizontal Distance (m)	Cylinder			
	CHBC	Yan et al. (2018)		
0.0	15	5		
0.5	8	22		
1.0	13	38		
1.5	17	47		
2.0	32	58		
2.5	52	89		
3.0	68	103		
3.5	69	122		

The CHBC achieved an average cumulative RMSE of about 25 mm which was lower than the 47 mm of Yan et al. (2018), when the sensor height was 1.00 m. Yan et al. (2018) also had a steep increase in error for objects farther than 1.5 m from the laser sensor. The CHBC on the other hand had a low variance in RMSE with an increasing distance from the sensor. This shows that CHBC reduced RMSE by 46% for canopy width measurements.

2.4.2 Second Dataset Analysis

The quality of the dataset and hence, the performance of CHBC was also affected by the shape of the objects used. The regular objects (cylindrical, spherical and cuboids) used in Yan et al. (2018) provide definitive measurements against which the performance of the system can be tested but a better measure of performance can be obtained by using objects that are more representative of plant canopy shapes. In contrast, the second experimental setup tested the limitations of CHBC with respect to sensor height, while using a different set of objects. Table 2-5 and Table 2-6 show the RMSE in the width calculations made by the CHBC with the second experimental setup with respect to the sensor height and horizontal distance from the laser, respectively. The RMSE was measured for 5 sensor heights, 7 horizontal distances from the laser sensor, and 4 target objects.

The trend of an increasing sensor height resulting in improved measurement accuracy, obtained from the previous results, reached a point of diminishing returns (Table 2-5). The RMSE values tended to remain constant and even increased for increasing sensor heights. The ‘Plant Group-2’ had the lowest average RMSE of 19 mm at a sensor height of 2.0 m while ‘Plant Group-1’ and ‘Plant Group-3’ had their lowest mean RMSE values of 44 mm and 28 mm at sensor height of 2.5 m. The sensor height did not seem to affect the RMSE for the ‘Regular Object’. Greater sensor heights resulted in larger distances between successive laser beams (Sun et al., 2017). This means that the laser is more likely to miss the edges of the target objects which causes higher RMSE values. However, compared to the actual object sizes, these RMSE values were very small and could be ignored when the measured dimensions were converted to canopy volume for managing spray outputs.

Table 2-5: The RMSE of X direction (width) measurements across all horizontal distances of objects from the laser sensor (0.5, 1.0, 1.5, 2.0, 2.5, 3.0, 3.5 m) for five sensor heights.

Sensor Height (m)	RMSE in X Direction (mm)			
	Plant Group-1	Plant Group-2	Plant Group-3	Regular Object
2.00	50	19	38	10
2.25	71	34	46	28
2.50	44	32	28	15
2.75	54	26	47	14
3.00	58	35	46	21

The horizontal distance of the objects from the laser had no effect on the performance of the CHBC algorithm (Table 2-6) for all objects apart from ‘Plant Group-1’. This shows that the CHBC algorithm was able to effectively predict the dimensions of target object despite occlusion and distortion. There were slight increases in RMSE for objects placed at certain distances from the laser and this was due to the mirroring algorithm tending to over-estimate the dimensions of target objects. The regular object showed more consistent results which may be due to the regular object having a clear standard measurement compared to some human error in the manual measurement of irregularly shaped artificial plants.

Table 2-6: The RMSE of X direction (width) measurements across all sensor heights (2.00, 2.25, 2.50, 2.75, 3.00 m) for seven horizontal distances of objects from the laser sensor.

Horizontal Distance (m)	RMSE in X Direction (mm)			
	Plant Group-1	Plant Group-2	Plant Group-3	Regular Object
0.5	13	8	43	7
1.0	32	22	50	12
1.5	49	49	16	17
2.0	65	40	54	21
2.5	49	23	36	21
3.0	83	26	45	21
3.5	70	21	37	24

The clustering algorithm used was always able to identify individual plant canopies irrespective of the height of the sensor or the number of scans registered. There was also very little difference in the RMSE of measurements made with a single scan compared to three registered scans (Table 2-7). The registration of multiple scans, which would be time-consuming, was thus, not required. The removal of the distortion through mirroring was dependent on the height of the sensor and the quality of the dataset. To obtain accurate estimations, at least half of the plant canopies must be free from occlusion, which depends on row spacing and the height of the plant canopies.

Table 2-7: Comparison of RMSE with a single scan and three registered scans. The RMSE of X direction (width) measurements across all horizontal distances of objects from the laser sensor (0.5, 1.0, 1.5, 2.0, 2.5, 3.0, 3.5 m) for a sensor height of 1 m.

Target Object	RMSE in X Direction (mm)	
	Single Scan	Three Scans
Artificial Plants	53	42
Toy Ball	16	13
Basketball	21	18
Box	36	34
Cylinder	17	15

2.4.3 Optimal Sensor Height Calculation

The optimal sensor height for the best performance is dependent on the row spacing, number of plants in a row (range required), and the average plant height as shown in Figure 2-6 (Sun et al., 2017).

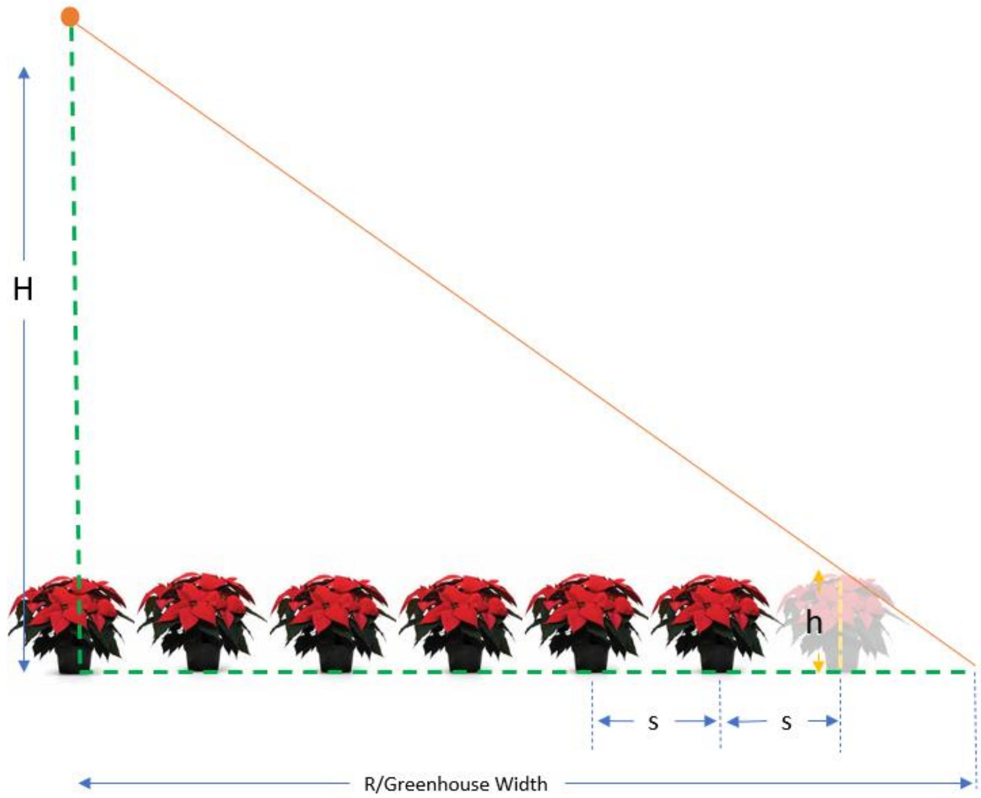

Figure 2-6: Deriving the optimal sensor height as a function of range, row spacing and average plant canopy height.

$$\frac{H}{R} = \frac{h}{s} \tag{2.7}$$

$$H = \frac{h}{s} R \tag{2.8}$$

Where, 'H' is the sensor mounting height (m)

'R' is the distance between two plants at two ends of the row (m)

'h' is the average plant height (m)

's' is the center to center plant spacing (m)

The general shape and the area of the plant canopy that needs to be visible to the laser sensor affect the optimal sensor height. Equation 2.8 is based on at least half of the plant canopy being visible to the laser for CHBC to perform well, assuming the container grown plants have symmetrical shapes. Using Equation 2.8, the optimal height for ‘Plant Group-1’ and ‘Plant Group-3’ was about 2.5 m from the ground (R = 4.00 m; h = 0.32 m; s = 0.50 m) which is confirmed by the results that show the lowest RMSE at a sensor height of 2.5 m. For the ‘Regular Object’ the optimal sensor height is about 2.75 m (R = 4.00 m; h = 0.34 m; s = 0.50 m) for which the RMSE value was the second lowest measured and for ‘Plant Group-2’ the optimal sensor height was about 1.7 m (R = 4.00 m; h = 0.21 m; s = 0.50 m) and the lowest sensor height of 2 m showed the lowest RMSE results.

2.5 IMPROVEMENTS

The system can be further improved by overcoming a few limitations. The CHBC algorithm, in the case of two overlapping plant canopies, might over/under-estimate plant canopy dimensions since the points that lie in the region of overlap may be assigned to either plant canopy. The removal of ground points can be automated as opposed to the current solution where the user has to manually measure the distance from the laser to the ground and input the value into the program. The mirroring method used to estimate the shape of the occluded or distorted side of the plant canopy assumes that plant canopies are symmetrical which is not always the case. Hence, implementing a way to predict the overall dimensions of plant canopies with limited information through training models could potentially lead to more accurate measurements. An alternative could also be the combining of multiple scans from multiple angles if it is economically feasible.

CHBC increased the range that a single laser sensor could cover and accurately estimate plant canopy dimensions. Ultimately, it might have potential to be used for applications other than determining spray volumes such as plant phenotyping, and plant health monitoring. Heun et al. (2019) used laser data from two sensors to characterize plant canopies in the field for plant phenotyping. However, they only covered a total area of about 3.5 m. Sun et al. (2017) measured the maximum height of individual cotton plants for phenotyping purposes. However, they also covered a limited area of about 1.5 m using a single sensor. This project has demonstrated that with the use of CHBC, a single laser sensor can measure a total area of 7 m (3.5 m either side of the sensor) with an RMSE of 25 mm. This can increase the area covered by a single laser with a comparable accuracy and reduce the amount of time required to map large areas. The quality of the dataset begins diminishing significantly beyond 7 m as it becomes increasingly sparse and noisy.

2.6 CONCLUSIONS

To improve variable-rate spraying in greenhouses, this study proposed new approaches to improve canopy characterization. This was done with the introduction of a point cloud data processing algorithm and an evaluation of mounting height of the laser sensor. The processing algorithm improved the plant canopy measurement accuracy over a previously reported effort (Yan et al., 2018). A 46% measurement error reduction, in terms of root mean square error (RMSE), was achieved by effectively isolating individual targets from the dataset, removing distortion, and estimating the occluded portion of the plant canopies. The improvement was largely due to more accurate measurement of farther away plants where less point cloud data and more occlusion was observed.

Sensor height did affect the measurement performance, as reported by Sun et al. (2017), while using either the Yan et al. (2018) methodology or the processing algorithm proposed in this research. The latter method was more accurate and robust at different sensor heights. In comparison, the lowest average RMSE of the plant canopy width measurements were achieved when the sensor was placed at a height of 1 m from the top of the canopies - 25 mm for the processing algorithm compared to the 47 mm from Yan et al. (2018). The proposed processing algorithm was also more reliable in accurately measuring plant canopies when the height of the sensor was determined by calculating an ‘optimal sensor height’ that was dependent on the height of the plants, the canopy to canopy spacing, and the total range/greenhouse width to be measured.

Chapter 3: An Offline Variable-Rate Sprayer System for Greenhouse Applications

3.1 ABSTRACT

Conventional fixed-rate spray systems used to apply pesticides inside greenhouses are wasteful, with large off-target losses and over-spraying of plant canopies. Variable-rate sprayer technology has resulted in spray savings of 45% inside greenhouses even with a limited accuracy in canopy characterization (Yan et al., 2019). Further savings can be made if the canopy characterization is improved. This project incorporated an algorithm that improved measurements of canopy dimensions (Chapter 2) coupled with a convex hull methodology into a system designed by Yan et al. (2019). The purpose of this addition was to improve the measurement of plant canopy dimensions and volumes, which are used to calculate spray rates. However, this required modifying the Yan et al. (2019) system from an inline operation to an offline one, because the algorithm used required extensive computing time. The modifications made were tested by visualizing the location of nozzle activation. The activation of the nozzles was found to begin spraying within 7.21 mm of the edges of plant canopies. The processing algorithm (Chapter 2) with the convex hull methodology was found to improve on the Yan et al. (2019) methodology, recording an overall mean accuracy of 81% compared to 66% by Yan et al. (2019). The improvement in volume estimation resulted in a reduction in spray volume used by 15%. The spray coverage performance of the modified offline spray system was tested in a greenhouse environment against the Yan et al. (2019) system and a conventional fixed-rate spray system. The offline system significantly reduced spray coverage at the edges of plant canopies while meeting the recommended spray coverage percentages. The tops and bottoms of canopies that were grouped close together had similar percentage coverage for all three systems. The coverage

in the bottoms of plant canopies was reduced below recommended values for the offline system. The reduction in coverage was compensated by a density of droplets, which was sufficient for pest prevention. The offline system achieved an 86% reduction in spray volume compared to a conventional spray system and improved the efficiency of the Yan et al. (2019) variable-rate spray system by 53%.

Keywords: Automation, Application Technology, Controlled Environment Plant Production, Convex Hull, LiDAR, Offline Operation, Precision Agriculture

3.2 INTRODUCTION

Traditional pesticide application systems using fixed rate sprayers are wasteful, have large off-target loses, and tend to over-spray canopies. This excess of harmful chemicals can be detrimental to the environment and worker safety, and it can become a financial drain because the grower is paying for more chemicals than are necessary. Run-off from greenhouses has been documented to exceed safe environmental limits from both flower and vegetable production facilities (Roseth and Haarstad, 2010). The chemical concentrations in the runoff also tended to exceed those from agricultural runoff for the majority of compounds measured (Roseth and Haarstad, 2010). Prolonged exposure to harmful chemicals in pesticides can pose serious health risks for workers (Damalas and Eleftherohorinos, 2011). Semchuk et al. (1992) have also suggested that pesticide exposure can result in workers being more prone to Parkinson's disease. Greenhouses have the added drawback of being contained systems that are slow to vent, thus exposing workers to spray cloud drift for extended periods of time (Siebers and Mattusch, 1996). Therefore, it is essential to improve existing chemical application systems.

Researchers have proposed methodologies to improve spray efficiency for field applications, such as orchards and vineyards, as traditional spray technologies are wasteful and have low deposition efficiency (Giles et al., 2011; Pergher et al., 1997; Seiber et al., 1993). Seiber et al. (1993) measured the spray deposition from dormant spraying of diazinon and concluded that 88% of the pesticide hit the peach orchard floor rather than the canopies. Pergher et al. (1997) compared chemical application techniques in a vineyard and found that 37% to 62% of the spray volume applied did not get deposited on the leaves of the target canopy. Sánchez-Hermosilla et al. (2011) observed that only about 50-66% of the spray hit the tomato canopies while the rest was lost to the ground. The efficiency of these systems can be improved significantly by using a variable-rate sprayer (Escolà, 2010; Giles et al., 2011; Jeon and Zhu, 2012; Shen et al., 2017; Chen et al., 2012; Yan et al., 2019; Zhu et al., 2017). The principle of the variable rate sprayer is to detect the presence of a canopy; measure its characteristics, such as volume and density; and control the spray volume of each nozzle based on those calculations. Chen et al. (2012) showed a reduction in chemical use by 47-73% when implementing a variable-rate sprayer in orchards. Giles et al. (2011) observed savings in spray volumes between 15% and 40% in orchards. Zhu et al. (2017) reduced spray volume by up to 77.6% using a laser-guided variable-rate sprayer in ornamental nurseries. Shen et al. (2017) also managed to reduce spray volumes while improving sprayer coverage by up to 55% in a commercial nursery.

In greenhouse boom spray systems, the spray efficiency is improved by operators manually changing spray outputs to match plant sizes. They normally mount a multi-nozzle manifold with 4 to 5 different size nozzles at each position, and manually select the nozzles as needed. This process is time-consuming, not precise, and prone to human error. The same principle of the variable-rate sprayer that is used in the field can be utilized in greenhouses to improve spray efficiencies, but it must be adapted. Sánchez-Hermosilla et al. (2013) observed upwards of 30% reduction in spray volume for greenhouse tomato crops by varying the application rate depending on Plant Row Volume (PRV), which was measured manually. This canopy characterization process can be automated by using a LiDAR/laser sensor. Yan et al. (2019) placed a laser sensor onto a travelling spray boom to determine canopy characteristics from above. The resulting three-dimensional map of the canopies was then used to characterize them to determine the spray volume required from each nozzle. The mean spray volume savings observed were around 45% even though the measurements made from the laser sensor had limited accuracy. The dataset obtained became increasingly limited and noisy as the distance from the laser sensor increased due to problems of occlusion. Only one side of a plant canopy was visible to the laser sensor, while the rest of the canopy was hidden (Yan et al., 2018). Hence, with an improved accuracy in the canopy characterization, further savings in spray volume can be achieved. The canopies can be characterized better by introducing a point cloud data processing algorithm (Chapter 2).

The canopy characteristics, such as volume and density, that are used to determine the required spray rate can be determined in a number of ways. Yan et al. (2019) and Chen et al. (2012) calculated them by assuming each point in the LiDAR point cloud dataset to be a 'bar' of unit length and width. The height of each 'bar' was the distance of the point from the ground (Yan et al., 2019) or to the assumed center of the tree canopy (Chen et al., 2012). The cumulative volume of these 'bars' was used to determine spray volume. The density of a section of the point cloud was calculated as a ratio of the minimum volume of the cuboid that encompasses all the 'bars' to the cumulative volume of the 'bars' in the section. This approach did not consider intra-canopy density variations. This resulted in an overestimation of plant canopy densities (Yan et al., 2019), because canopies tend to be less dense at the edges, compared to the center, so the edges require less spray. To achieve more precise canopy volumes estimations, various methods can be incorporated such as a convex hull, segmented convex hull, cylinder-based modelling, as well as a voxel-based approach (Cheein et al., 2015; Chakraborty et al., 2019; Escolà et al., 2017; Lee and Ehsani, 2009). The approach used in this project was a 3D convex hull, which is computationally simple and provides a volume measurement that is closely correlated to manual measurements (Chakraborty et al., 2019; Lee and Ehsani, 2009).

The improvement in canopy characterization and volume and density estimation comes at the cost of computing time, which makes inline performance, in which operations are carried out synchronously, difficult. This project integrated the 3D convex hull with the system developed by Shen et al. (2017) and Yan et al. (2019), which was designed for inline operation. Hence, it needed to be modified for offline functionality, that is, sequential operations in which the laser sensor scanned the canopies on one run and then sprayed the canopies on a secondary run. This two-step process added a few complications because the position of the plant canopies in space was required to determine when to trigger the nozzles for the secondary spraying run. However, there is limited GPS functionality in indoor spaces such greenhouses, which makes it difficult to identify the exact location of plant canopies so only their relative position can be obtained. The location of canopies was detected by comparing point cloud datasets from the previous 'scan run' to the data being collected during the 'spray run' using a similarity index.

This project modified the spray system developed by Yan et al. (2019) to convert the system from an inline/real-time operation to an offline operation. A new Graphical User Interface (GUI) was rebuilt to facilitate the two separate operations of scanning and spraying and allow the user to specify operating parameters for greenhouses of varied dimensions and constraints.

The goal of this project was to improve spray volume savings while ensuring plant canopies were sufficiently covered with spray. Hence, the modified system was tested in a greenhouse environment to observe its spray coverage performance as well as its effectiveness in identifying targets and minimizing spray loss to the ground.

The objectives of this project were to:

- Modify the Yan et al. (2019) system to enable offline operation
- Improve the canopy volume estimations using a 3D convex hull approach
- Evaluate spray volumes determined for individual plants using the convex hull-based volume approach
- Evaluate the spray deposition over the plant canopy in a commercial production greenhouse using the modified offline system

3.3 MATERIALS AND METHODS

To better characterize plant canopies, a 3D complex hull methodology coupled with a processing algorithm (Chapter 2) was integrated into an existing system developed by Yan et al. (2019). The Yan et al. (2019) system retrofitted a conventional travelling spray boom commonly used for commercial greenhouses with multiple components. They included a 270˚ wide-range laser scanning sensor (UST-10LX, Hokuyo Automatic Co., Ltd., Osaka, Japan), an embedded computer, pulse-width modulated (PWM) solenoid valves and a PWM controller (Liu et al., 2014). The PWM solenoid valves were coupled with nozzles for a controllable spray rate. Custom software was developed by Yan et al. (2019) and implemented to extract the data from the laser and control the spray output for inline functionality. To integrate the 3D convex hull methodology and the processing algorithm (Chapter 2) into the Yan et al. (2019) system, certain modifications were required. All the hardware components, apart from the embedded computer, of the Yan et al. (2019) system remained unchanged. A laptop (Dell Latitude 3500, 2018, Dell Inc., Texas, USA) was used rather than an embedded computer. The software in the Yan et al. (2019) system was changed and this required converting the system from an inline to offline operation.

3.3.1 Offline Operation

Offline operation splits the operation of the system into a two-step process of scanning and spraying rather than doing them synchronously (inline). On the scan run, the laser sensor data was collected and stored in a file. The data was then processed offline and used to determine spray rates for each individual nozzle over the length of the travel path of the spray boom. The system was then run again to spray the plant canopies. The conversion to an offline operation involved three major elements: offline calculation of spray rates, redesign of the Graphic User Interface (GUI), and timing the activation of nozzles on the spray run.

3.3.1.1 Offline Spray Rate Calculation

A 3D map was generated from the laser data, processed (Chapter 2), and then used to determine the spray rates of each nozzle required for the 'spray run'. All calculations were done offline using a numerical computing platform (MATLAB R2019a ver. 9.6.0.1114505, MathWorks, Natick, Massachusetts, USA). Because the density of plant canopies varies within a canopy as well as between canopies, the intra-canopy spray rate should also be varied to achieve the most efficient use of spray volume. To determine the varying spray rates of individual nozzles over the length of the travel path, the 3-D map obtained from the laser data was split into segments along the sensor's travel direction. Each segment represented the spray rate required over a specific region of the map for an individual nozzle (Figure 3-1). The length of each segment was determined by how often the spray rate of the nozzles needed to be changed and the speed 'ν' (Equation 3.1). The width of each segment was determined by the area covered by each individual nozzle, which is dependent on nozzle spacing (Equation 3.2).

$$Length\ of\ a\ segment = 0.125s\ \times \nu \tag{3.1}$$

$$Width\ of\ a\ segment = Nozzle\ Spacing \tag{3.2}$$

Where, ν is the travel speed of the boom and 0.125 s is determined by the frequency at which the PWM solenoid valves can be switched, which is 10 Hz (100 ms).

Therefore, the spray rate was calculated every 0.125 s – a time interval slightly lesser than its maximum switching frequency.

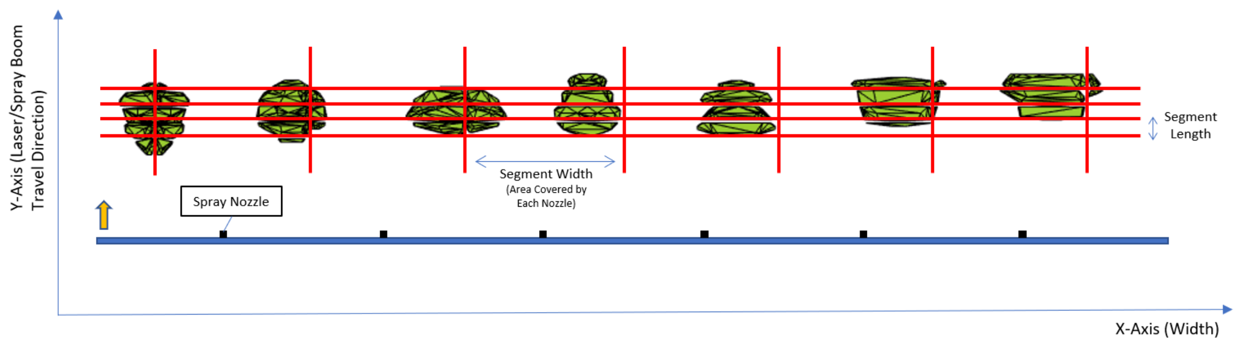

Figure 3-1: The processed 3-D data is split into segments to identify the sequence of varying spray rate required for each individual nozzle over the length of plant canopies.

The spray rate was controlled by varying the duty cycle of the nozzle. Duty cycle is the amount of time that each nozzle is required to be open to control its flow rate. It is calculated as a percentage value of the maximum flow rate when the nozzles are open continuously (Equation 3). The required flow rate in Equation 3.3 is calculated using Equation 3.4 (Shen et al., 2017; Yan et al., 2019).

$$Duty\ Cycle = \frac{Required\ Flow\ Rate}{Maximum\ Flow\ Rate\ of\ the\ Nozzle} \times 100 \tag{3.3}$$

$$Required\ Flow\ Rate = 60 \times w \times h \times v \times \rho \times \nabla \tag{3.4}$$

Where, ‘w’ is the range of a spray nozzle (width of a segment)

‘h’ is the maximum height of canopy that lies within a segment

‘ν’ is the travel speed of the boom and laser sensor

‘ρ’ is the density of the canopy that lies within a segment

‘∇’ is the spray rate required to effectively cover $1m^3$ of a canopy which is fixed at 0.13 (Jenkins and Hines, 2003; Yan et al., 2019).

The density (ρ) is calculated for each segment as a ratio (Equation 3.5):

$$\rho = \frac{Volume\ of\ canopy\ that\ lies\ in\ a\ segment}{Volume\ of\ cuboid\ that\ circumscribes\ the\ canopy\ segment} \tag{3.5}$$

The volumes of each canopy that fell in a segment were calculated by using a three-dimensional convex hull (Section 3.3.2.1). The volume of the circumscribing cuboid of a plant was calculated by finding the length, width and height of the canopy lying within the segment as shown in Figure 3-2. When a single nozzle was covering a width that has multiple plants of varying densities, the canopy with the highest density value was used.

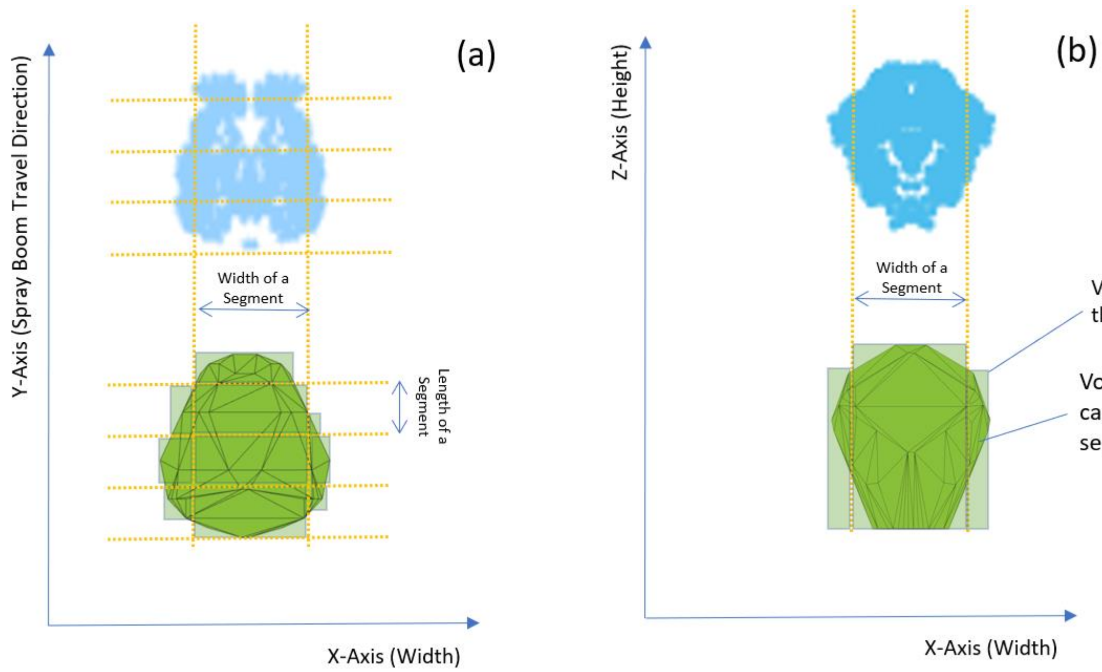

Figure 3-2: The calculation of the 'density' of plant canopies that lie within a segment. It is shown using the x-y axis (a) and the x-z axis (b)

The duty cycles for each segment in the whole dataset were calculated. The result was a sequence of duty cycles for each individual nozzle that represented the changes in spray rate over the length of the travel path of the spray boom.

3.3.1.2 Spray Control Graphic User Interface

The spray control GUI was redesigned to facilitate a two-step offline operation. It was used to obtain values from the user and ensure ease of operation. The GUI split the two operations into two tabs of the same window – the 'Laser Data Collection' tab and the 'Spray Application' tab.

Laser Data Collection Tab

The GUI Laser Data Collection tab was used to obtain inputs from the user that would be used to calculate spray rates offline. The inputs included travel speed, sensor height, sensor range, number of nozzles, nozzle spacing, and distance between first nozzles on either side of the sensor

(Figure 3-3).The travel speed was required to build a three-dimensional map of the whole region by assuming that the speed of the boom was constant and aggregating multiple two-dimensional scan lines. The sensor height information was used to remove ground points from the dataset. The sensor range was used to clip the dataset and use only the points that represented the region of interest and get rid of all other unnecessary points. The number of nozzles was required to determine the duty cycle of each nozzle. The nozzle spacing parameter was used to determine how to segment the dataset and identify which portion of the dataset fell under which specific nozzle and the area that each nozzle covered. The distance between the first nozzle on the left and right was used to identify the center of the region of interest (plants that need to be sprayed) and how to split the dataset into two halves, because there are two spray booms of equal length on either side of the laser sensor. The ‘Play’ icon, when clicked, turned on communication with the laser sensor and began recording data. The ‘Stop’ icon turned off the laser sensor and stored the recorded data in a file.

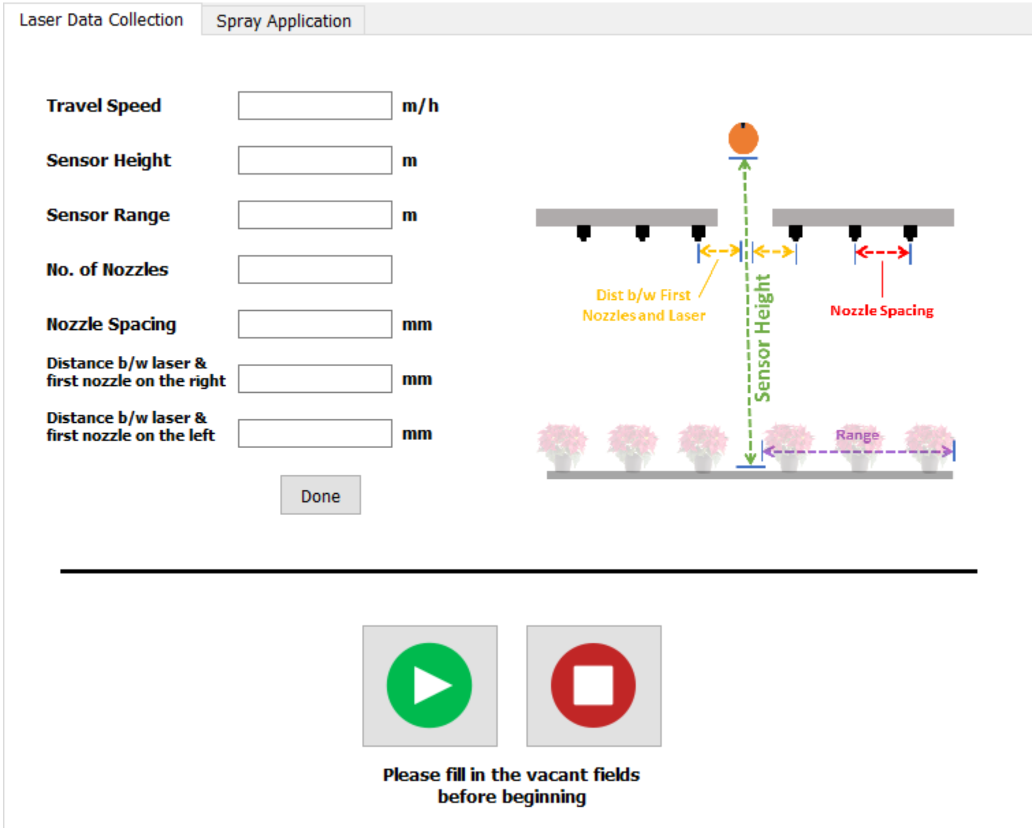

Figure 3-3: Graphical User Interface (GUI) to facilitate the easy operation of the spray system. It is also used to obtain certain information from the user required to process the data and understand the specifications of the system as well as the greenhouse.

Spray Application Tab

The GUI 'Spray Application' tab was used for the second step of the offline operation – the spray run. It provided the ability to test the nozzles to see if all nozzles were being triggered. The sliding bar to the right of the tag, 'Duty Cycle', enabled the user to test all nozzles at specific duty cycles to ensure their proper function prior to the spray run. The GUI also accepted an input for the distance between the laser and the nozzles (Figure 3-4). This distance was used to calculate the delay time required between the laser identifying the location of canopies in the spray run (Section 3.3.1.3) and the nozzles passing over them. The 'Play' icon, when clicked, turned on the laser sensor again. The laser sensor was used in the spray run to determine the location of plant canopies in the greenhouse to identify when to activate the spraying of the nozzles.

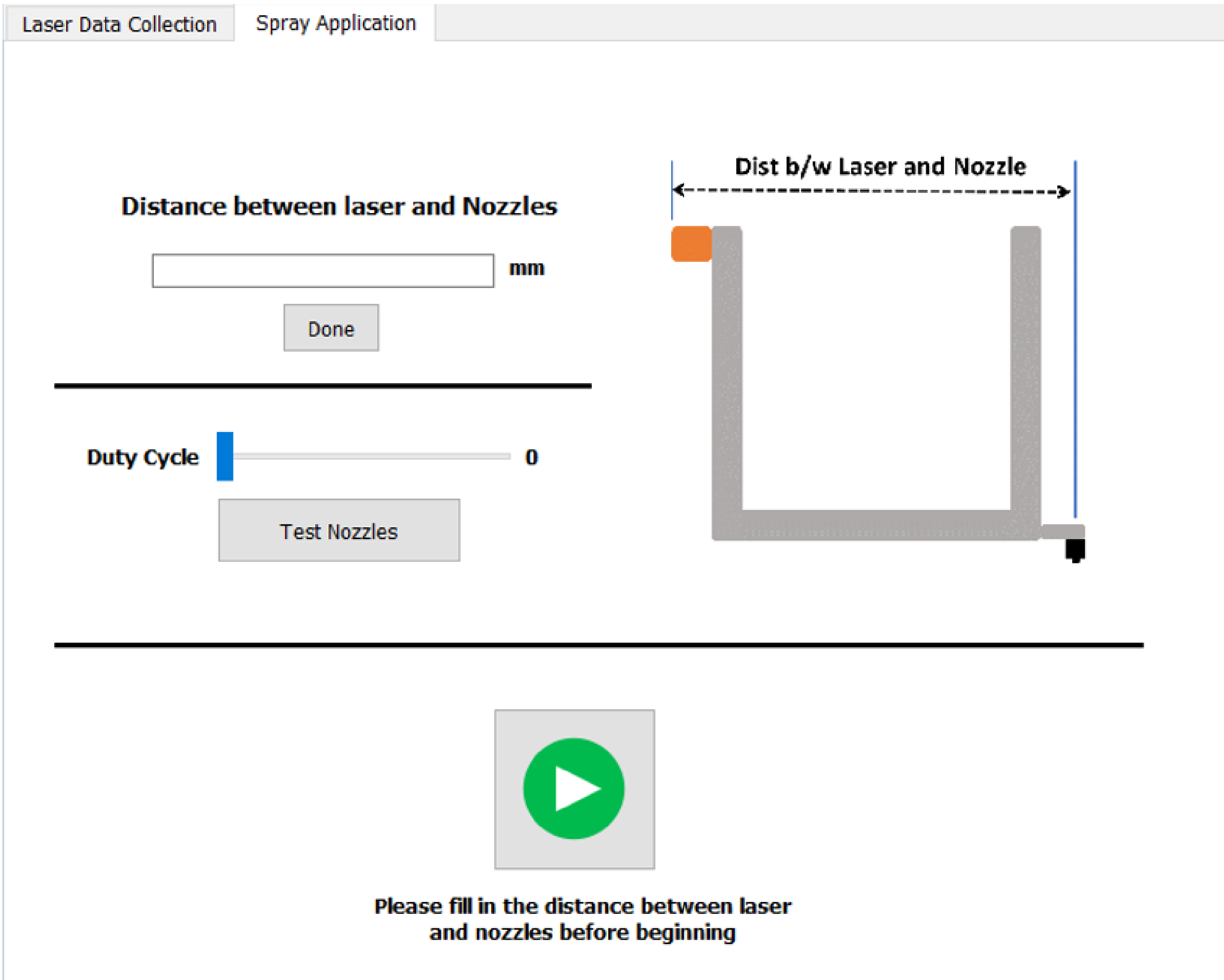

Figure 3-4: Graphic User Interface (GUI) designed for the spray run of the system. It enables the user to input parameters which assist in the timing of activation of the nozzles.

3.3.1.3 Nozzle Activation Timing

To spray plants precisely using the previously determined plant canopy density information, it was necessary to consider the positional offset between the sensor and the nozzles, and to detect the starting location of the spraying operation. The starting location was determined by using a similarity index to detect the presence of plant canopies. It compared the laser data being collected in the spray run to the previously recorded data from the scan run. If the two datasets were a match, it indicated that the plant canopies had been located.

Similarity Index

A similarity index provides a quantifiable measure when two datasets are compared to each other. The cosine similarity index was determined to be the easiest to implement as well as sensitive enough to show a significant drop-off when comparing dissimilar datasets. Cosine similarity is a measure of similarity between two vectors that uses the cosine of the angle between them. An index of 1 shows two identical vectors while 0 shows opposing vectors. The height data from the laser was used as the parameter to determine similarity (Equation 3.6). The first row of segments from the scanned dataset, which represented the starting location of plant canopies, was used as a reference vector. The first row of segments was represented by five scan lines from the laser sensor (five scan lines takes 0.125 s and it is assumed that the spray boom is travelling at the same speed as during the scan run (Equation 3.1)). Five consecutive scan lines were therefore taken from the laser and compared to the reference vector. If a similarity threshold of 85% was not met, the first scan line of the five was removed and the next one was added. The process repeated until the threshold was met, after which a new loop was executed where the program tried to achieve the highest possible similarity by replacing the earliest scan lines with new ones. Once the highest possible similarity was achieved, it assumed that the edge of the first canopy was detected and the duty cycle sequence was called with a delay time based on the distance between the laser sensor and the nozzles and the travel speed. The nozzle activation time and the time it took to identify the edge were accounted for in this delay time.

$$\cos\theta = \frac{\vec{a}.\vec{b}}{\|a\|\|b\|} \tag{3.6}$$

Where, $\vec{a}$ is the height data from the scan run

$\vec{b}$ is the height data from the spray run

Laser Alignment

Another factor that affected the nozzle activation timing in a practical scenario was the alignment of the laser sensor against the spray boom (Heun et al., 2019). Theoretically, it is assumed that the sensor scan line is completely parallel to the spray boom, but this is not the case when mounting the laser. In a greenhouse, when the sensor scans a length of close to 10 meters, this effect is amplified and can cause the laser to identify a canopy before it is actually in line with it or identify the canopy after it has crossed it, based on the uncompensated misalignment. This needed to be corrected because the performance of the whole system was dependent on the accuracy with which the canopies were located. Therefore, the error of the laser scan line was observed by scanning a straight row of objects with a straight edge (e.g. cardboard boxes). Ideally, the laser scan should have shown a straight line of objects but due to alignment issues there was a slight slope to the line. This slope was calculated, and depending on the distance of the canopy from the laser, a delay time was added or subtracted based on the tangent of the angle of slope.

3.3.1.4 Nozzle Activation Test

The timing of the activation of nozzles was a good measure of the performance of all the modifications made to the inline system (Yan et al., (2019)) for offline operations. It was evaluated using two experimental setups - one in a laboratory and the other in a commercial greenhouse (Casa Verde Growers, Columbia Station, OH). The ability of the system to detect the starting location of plant canopies and spray accuracy of the subsequent plants along the travel direction was tested in one experiment. The effect of the laser alignment was tested in a second experiment.

The nozzle activation was measured by using a shallow tray filled with arselite (Turface Quick Dry, Turface Athletics, Buffalo Grove, IL, USA) and obtaining a visual of the spray pattern (Figure 3-5). Arselite has preferred properties for the spray location detection as it: 1) changes color when wet (Figure 3-5(b)), making visual observation easier; 2) absorbs more water and has less surface runoff than water sensitive paper, which is commonly used for this type of study; and 3) allows for repeated measurements because the surface can be easily refreshed by removing the wetted arselite and resurfacing it with dry arselite.

The laboratory experimental setup consisted of placing one row of target objects along the travel direction and marking their starting edges. The edges of the objects were marked across the arselite tray so that errors in nozzle activation could be measured as the wet arselite provided a clear distinction of where the nozzles were activated. Four regular shaped objects with clearly-defined straight edges were used – 2 metal disks and 2 fiberglass objects. Four artificial plants were used as well, of which three were of similar dimensions while one had smaller dimensions. The four objects were placed 0.5 m apart from each other along the travel path and at a fixed distance of 1.5 m from the laser sensor. The distance between the nozzle and the laser sensor was 1.5 m. A single nozzle was used to simulate the performance of all the nozzles on the spray boom. It was located adjacent to the target objects, at a height of 25 mm from the arselite tray target and functioned at a pressure of 275 kPa. A flat fan nozzle (XR8001, TeeJet Co., Wheaton, IL, USA) was used to get a thin spray pattern. The distance between the nozzle being activated and the red chalk line on the arselite that represented the edges of the objects was measured.

Observations were made for the four regular shaped objects as well as the four artificial plants, with five repetitions for each. The spray system travelled at a speed of 0.116 m/s.

A similar experiment was conducted in a commercial greenhouse with a few adjustments. The spray boom system used had two spray wings of equal length, either side of the laser sensor (UST 10-LX, Hokuyo, Osaka, Japan). The wing had 20 nozzles (XR80015, TeeJet Co., Wheaton, IL, USA) coupled with PWM solenoid valves (Capstan Ag Systems Inc., Topeka, KA, USA), spaced 533.4 mm apart, covering a total distance of 9 m. The solenoid valves were controlled by a PWM controller (Liu et al., 2014). The PWM controller and the laser sensor were connected directly to the laptop. The boom and the laser sensor traveled at a constant speed of 0.224 m/s. Five objects were placed in a row along the travel direction, and readings were taken by placing the row of objects at three different distances from the laser (1.5, 2.5, 3.5 m). The objects used were all regular shaped boxes. Three repetitions were run for each position of the row of objects.

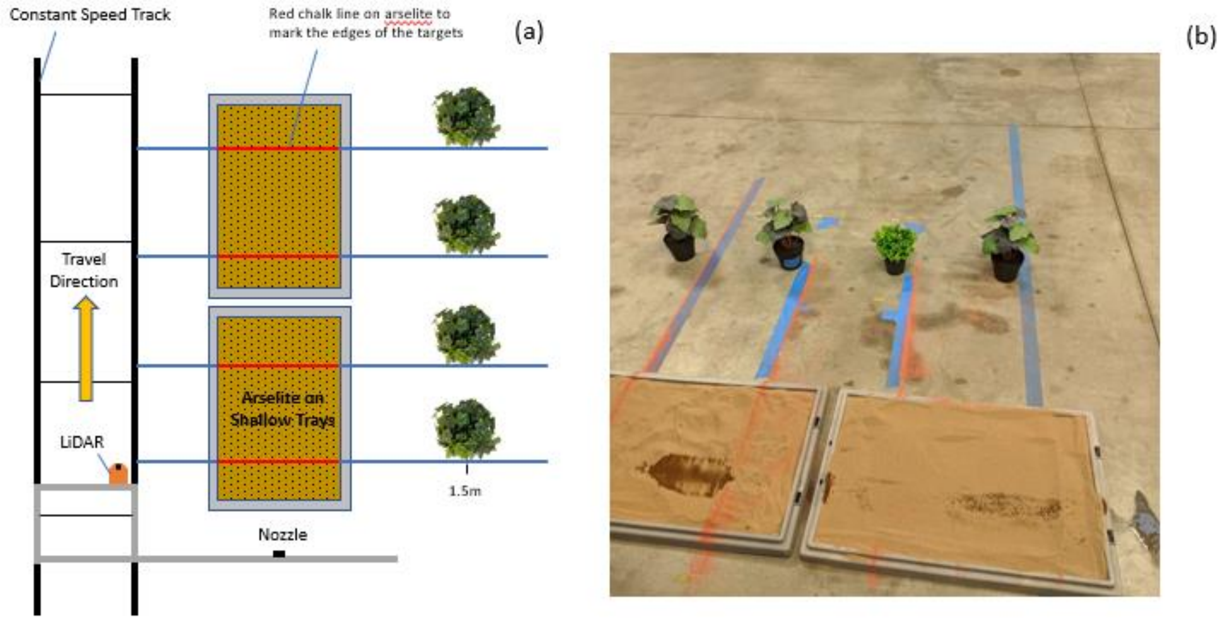

Figure 3-5: (a) The experimental setup to determine the accuracy in the activation of nozzles once canopies have been detected. (b) The spray pattern was visualized on the arselite tray and its deviation from the edge of the canopy (marked by red chalk on the arselite) was measured.

3.3.2 Canopy Volume Estimation Improvement

A 3D convex hull method was used to determine the volumes of plant canopies. The contours of plant canopies were considered rather than just the elevation data from the laser data (Yan et al., 2019; Chen et al., 2012). The volume data was used to calculate density and spray rate.

3.3.2.1 Convex Hull Method

A convex hull is the smallest convex polygon containing a given set of points. In 3D space, it creates a bounding surface that follows the contour of all the external points that represent a plant canopy. The volume that this surface encapsulates then gives us the volume of the canopy. This convex hull volume can be used for individual plant canopies in the dataset by using a 'clustering' algorithm, which isolates canopies from the laser dataset (Chapter 2). The convex hull approach was used to identify volumes of canopies that were present within a segment of the split laser dataset to calculate spray rates offline. A built-in function on a numerical computing platform was used to generate the convex hull and calculate its volume (‘alphaShape’, Copyright 2013-2015, The MathWorks, Inc.). The ‘alphaShape’ function creates a polyhedron that envelops a set of 2-D/ 3-D points. To find a convex hull, the alpha angle is set to infinity.

The edges of plant canopies are less dense and require lower spray volume than the center. This intra-canopy density variation is represented when using the convex hull method because it follows the three-dimensional contours of the plant canopy. When split along the travel direction, the density values and the subsequent spray rates calculated will be lower at the edges of the canopy (Figure 3-6).

Through laboratory evaluations, it was found that the density values at the extreme edges of the canopy can result in very low required spray rates and, therefore, low duty cycles – in the range of 2-15%. The PWM solenoid valves have limitations in their performance for duty cycles lower than 20% (Gu et al., 2011) that may result in the edges of the canopy not being sprayed with enough chemical to prevent disease. Alternatively, one can use nozzles with lower spray rates to increase the duty cycle values obtained because the duty cycle is inversely proportional to the ‘Maximum Flow Rate’ of the nozzle (Equation 3.3). Therefore, nozzles which had a maximum flow rate of 1.5 L/min (0.40 GPM) at 275 kPa (XR8004, TeeJet Co., Wheaton, IL, USA) were replaced by nozzles that had a maximum flow rate of 0.5625 L/min (0.15 GPM) (XR 80015, TeeJet Co., Wheaton, IL, USA) at the same line pressure. This scaled duty cycle values and achieved a more precise spray rate control for the intra-canopy variation in density.

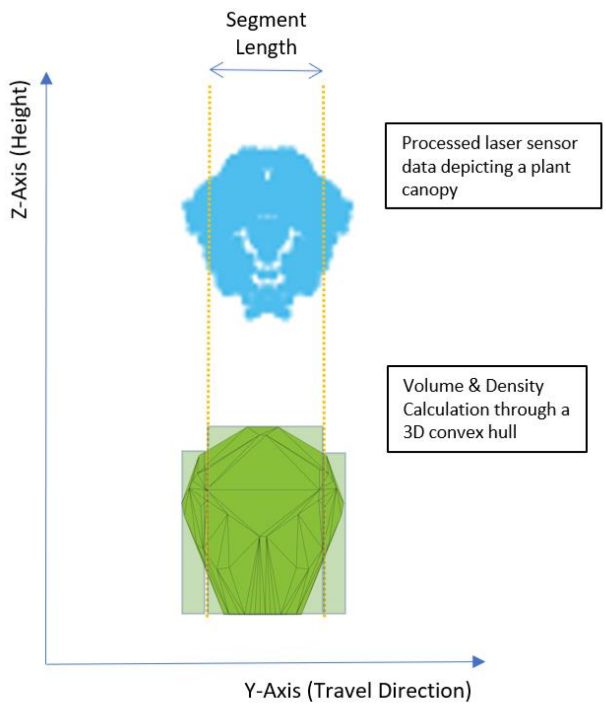

Figure 3-6: The convex hull approach calculates volumes by following the contours of the whole canopy. The density calculated for the edges of the canopy will therefore be lower than the in the middle, which is denser.

3.3.2.2 Canopy Volume Estimation Evaluation

The performance of the convex hull approach was first evaluated using the dataset obtained by Yan et al. (2018). It consisted of 5 rows of object – 4 rows of regular objects (toy ball, basketball, box, cylinder) and 1 row of irregular objects (Plant Group-1). The objects were spaced 0.5 m apart both between and within rows. The dimensions of the objects are given in Table 2-1. A laser sensor (UST 10-LX, Hokuyo, Osaka, Japan) was placed on a constant speed track at a height of 1 m from the top of the objects. The travel speed was 0.447 m/s. The volume of the regular shaped objects and artificial plants were measured manually and compared with the volume obtained through the convex hull approach. The use of regular shaped objects provided a clear standard against which the performance could be tested. Artificial plants were used because they maintain their size and shape over time and can be used multiple times.

The performance of the system was further evaluated in a commercial greenhouse. The laser sensor was placed at a height of 3 m from the ground and the spray boom travelled at a speed of 0.178 m/s. A sensor height of 3 m was chosen based on our previous effort (Chapter 2). The average plant height of the three varieties was 305 mm and the center to center width was 500 mm since the big canopies had a width of around 408 mm, with a range of 4.5 m. Three varieties of plant canopies of different volumes were manually measured – big, medium, and small. The average dimensions of the five plant canopies of each variety are shown in Table 3-1. The plants were placed adjacent to each other at varying distances from the sensor.

Table 3-1: Dimensions of plant canopies used to test the performance of the convex hull approach in the greenhouse. Standard deviations are given within the parenthesis.

Canopy Type	X (Width) (mm)	Y (Length) (mm)	Z (Height) (mm)
Big	408 (30.3)	396 (13.4)	368 (8.4)
Medium	332 (42.7)	326 (8.9)	302 (10.9)
Small	214 (23.0)	230 (29.2)	246 (20.7)

3.3.3 Spray Volume Evaluation

The convex hull method's ability to improve variable spray rates within plant canopies was tested to see whether it resulted in a meaningful reduction in spray volume. It was compared to the approach used by Yan et al. (2019). The evaluation was carried out in a laboratory setting using three groups of plants of different dimensions (Table 2-2) and a single nozzle. There were seven plants in a group that were placed at incremental distances from the laser (0.5, 1.0, 1.5, 2.0, 2.5, 3.0, 3.5 m).

Proper nozzle flow rate is important in evaluating PWM-solenoid-valve controlled operation due to the limited performance when the duty cycle is less than 20%. Two nozzles with different flow rates were evaluated to determine which performed closest to its theoretical volume (Table

3-2). The nozzle with a high flow rate,1.5 L/min, (XR 8004, TeeJet Co., Wheaton, IL, USA) and, subsequently, lower duty cycles had lower spray volume output than was theoretically expected and was unreliable in its performance. Most duty cycles calculated were below 20%. The PWM valves did not open for duty cycles below 10% and performed unreliably for duty cycles below 20% (Gu et al., 2011). This resulted in spray volumes that were closer to theoretical volumes, calculated using Equation 3.7, but only because the nozzle failed to open for most of its operation; thus, the spray will not reach all parts of the plant canopy, and result in poor spray coverage. Measured volumes are always higher than theoretical volumes during normal operation. The nozzle with a lower flow rate of 0.5625 L/min (XR 80015, TeeJet Co., Wheaton, IL, USA) had higher duty cycles and therefore, a more reliable performance, producing spray volumes higher than the theoretical values which is more in line with the normal operation (Figure 3-7), where the measured spray output is much higher than the theoretical spray output. The higher measured spray volumes are due to mechanical limitations of the PWM solenoid valves not being able to open and close fast enough (Yan et al. 2019). There was also some excess dribble once the nozzles were turned off. Based on the evaluation of the two nozzles, the lower flow rate nozzle, 0.5625 L/min, was chosen because of its more reliable performance.

Table 3-2: The lower flow rates and higher duty cycles result in more reliable outputs above theoretical volumes. The spray volumes measured from two different nozzles with different flow rates are compared. Standard deviations are in parenthesis.

Parameters	Nozzle Flow Rate – 1.5 L/min	Nozzle Flow Rate – 0.5625 L/min
Mean Measured Vol (ml)	2.02 (1)	7.48 (1.8)
Theoretical Vol (ml)	2.51	2.57

$$Theoretical\ Spray\ Volume(ml) = \sum_{i=1}^{n}\left(Duty\ Cycle_i \times Maximum\ Flow\ Rate\ ({}^{ml}/_{s})\right) \times 0.125s \qquad (3.7)$$

Where, 'n' is the number of segments in the calculated sequence of duty cycles

0.125 s is the the time between successive duty cycles

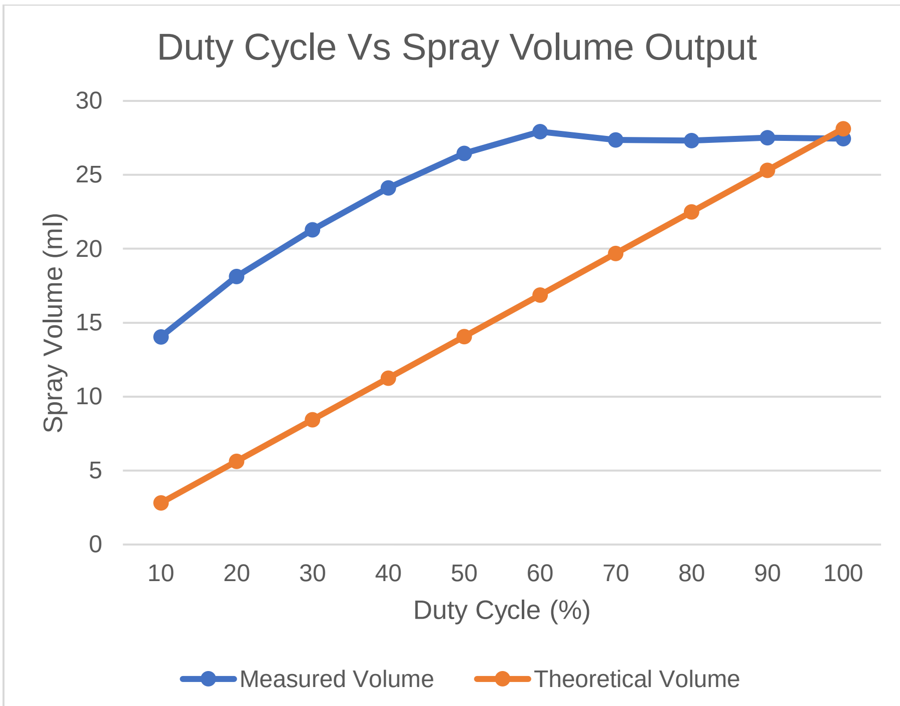

Figure 3-7: The measured volumes are consistently higher than theoretical volumes due to mechanical limitations of the PWM valves. The comparison between theoretical volume and the measured volume at varying duty cycles for a nozzle with a flow rate of 0.5625 L/min.

The spray volume output of each of the seven nozzles was regulated by sending their respective duty cycle sequences to the PWM controller (Liu et al., 2014). The lab setup was restricted to a single nozzle; therefore, the spray volume output of the seven nozzles was measured one at a time. The spray output was collected using a container that covered the whole area of the nozzle. Water was used as a safe alternative to chemical spray. The water collected was then measured using an electronic scale (PG2002-S, Mettler Toledo, Columbus, OH, USA), with a resolution of

0.01 g. The process was repeated five times for each of the seven nozzles and for both of the plant canopy volume determination methods mentioned above.

3.3.3 Spray Coverage Test

The spray coverage achieved by the offline spray system was tested in a commercial greenhouse using real plant canopies. The laser sensor was mounted at a height of 3 m from the ground, scanning the plants from above. The sensor height was determined using the method described in Chapter 2 where the average height of the three canopies (Table 3-3) was 328 mm, the canopy to canopy spacing was considered to be 500 mm as the big canopies had a width of around 464 mm and the range/width of the greenhouse was 4.5 m. The largest canopies were considered for the canopy to canopy spacing because the tight spacing of smaller plants would result in a sensor height that would cause large errors in characterization (Chapter 2). The spray boom and the laser sensor were travelling at a constant speed of 0.178 m/s. Nozzles with a flow rate of 0.5625 L/min at a pressure of 275 kPa were used and any duty cycles below 20% were scaled to 20% to ensure that the PWM valves turned on and performed reliably. A flow meter (SM8001, IFM Efector Inc., Essen, Germany) was connected to the boom to measure the spray volume output of the system.

Spray coverage on the plant canopies was observed using water sensitive paper (WSP). WSP has been widely used to determine spray coverage (Chen et al., 2013; Salyani et al., 2013; Sinha et al., 2020; Wu et al., 2019; Xiao et al., 2018). Strips of the WSP were placed on the edges of selected plant canopies along the travel direction as well as on the top and bottom of other target plants. A total of 16 canopies were selected to test spray coverage performance. Figure 3-8(a) illustrates the experimental layout of the plants and locations of the WSP targets. Three different sizes of plant canopies were used (Table 3-3) to test the performance of the system against canopies of varying volumes. Ten WSPs were also placed on the ground to monitor the ability of the system to stop spraying when there was no plant. The longer targets (G1, G2, … G6) were used to test whether the nozzles were activated and deactivated at the right times, while the small targets (G7, G8, G9, and G10) were used to test whether the right nozzles were activated (Figure 3-8(a)). Data from three spray volume determination methods were collected - the modified, offline system discussed in this project; the Yan et al. (2019) system; and a conventional fixed-rate spray system. Three replications were performed for each of the three methods. The sprayed WSP were then analyzed using an imaging software that determined spray coverage percentage and droplet density, among other values (Zhu et al., 2011).

Table 3-3: Dimensions of the three varieties of plant canopies used for the spray coverage test in the greenhouse. Standard deviations are in parenthesis.

Canopy Type	Width (mm)	Height (mm)
Big	464 (68)	480 (54)
Medium	271 (36)	299 (16)
Small	174 (10)	205 (28)

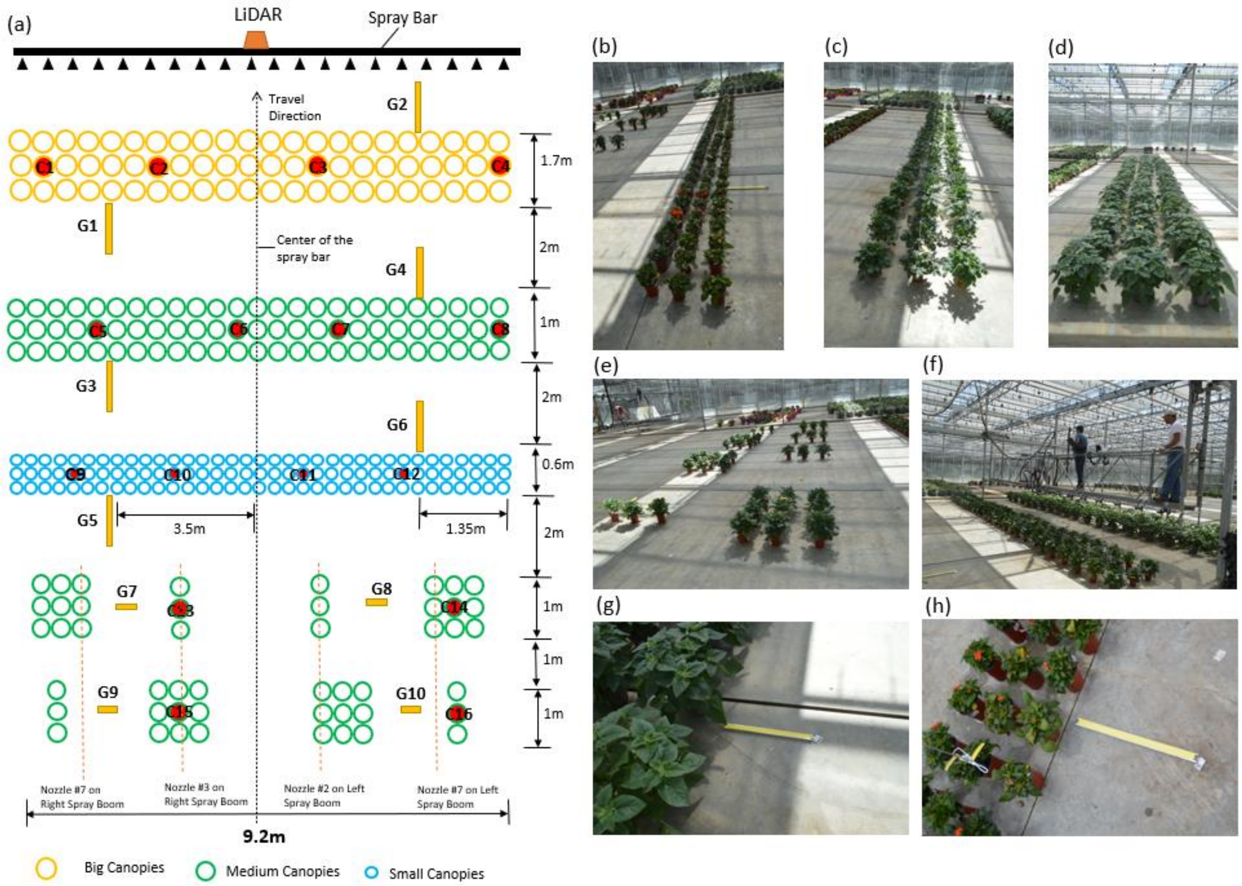

Figure 3-8: (a) Experimental design to test the spray coverage of the offline spray system in a greenhouse environment. (b) Three rows of small plants. (c) Three rows of medium sized canopies. (d) Three rows of big canopies. (e) Scattered pattern of medium canopies to test whether the right nozzles are being triggered. (f) Spray boom travelling over the experimental setup. (g)

3.4 RESULTS AND DISCUSSION

3.4.1 Nozzle Activation

3.4.1.1 Lab Experiment

The control of spray location was found to have good accuracy using the four objects placed in a row along the travel direction (Figure 3-9). The nozzle was activated within 7 mm of the edge of the canopies based on the mean of the error of all rows., with a standard error of 1 mm. The nozzles were always activated before the edge of the objects. The error in nozzle activation depended on two factors – the accuracy with which the similarity index detected the starting location of target objects and the speed of the system. The starting location of the objects determines when the sequence of duty cycle data generated through offline processing is sent to the PWM controller to trigger the nozzles. The speed of the system affects nozzle activation because it is assumed to be constant and identical for both the scan run and spray run. If there were consistent discrepancies in the speed between the two runs, there would be an error accumulation, where an increasing travel distance would result in an increasing error with each object. The error in Object 1 showed that the target object location was detected with an accuracy of 7 mm. Object 2 had a mean error of 10 mm, Object 3, 3 mm, and Object 4, 8 mm. The error was not accumulative for each object. Therefore, the assumption of identical speeds for both runs was found to be reasonable under the experimental condition

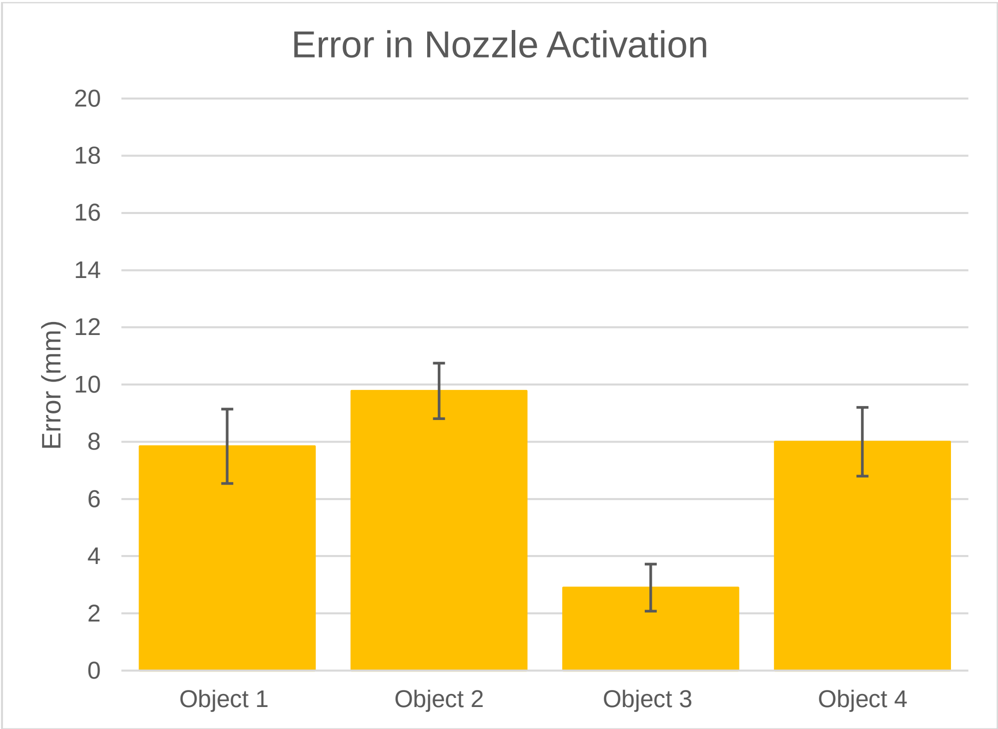

Figure 3-9: The error in location of activation of spray nozzles. All errors were below theoretical limits. There was no cumulative error in the activation with an increasing travel distance (signified by the lack of an increasing error with each row).

The theoretical maximum error in activation must lie within the distance calculated by Equation 3.8.

$$Error \leq (0.125 \times Travel\ Speed)\ \mathrm{mm} \tag{3.8}$$

Where 0.125 s is the time it takes for the laser sensor to send 5 scan lines.

The formula is the same as the length of a segment in the density calculations mentioned previously. This error exists because the algorithm splits the entire dataset into segments (depicted by the yellow lines in Figure 3-10) from the starting edge of the first object. Hence, the subsequent edges of multiple rows of objects may not lie perfectly at the start of a segment (Figure 3-10(a)) and may even have a small portion of the edge in the segment, but this is enough for the nozzle to be activated because there is an object present in the segment. The error in nozzle activation is directly proportional to the travel speed of the spray boom. Hence, the higher the speed of the spray boom, the larger the potential error in nozzle activation. The errors in all rows for the laboratory experiment were within the theoretical limit of 14.5 mm calculated for this test using Equation 3.8. Therefore, the assumption of a constant speed was also found to be reasonable and any inconsistences in travel speed were insignificant.

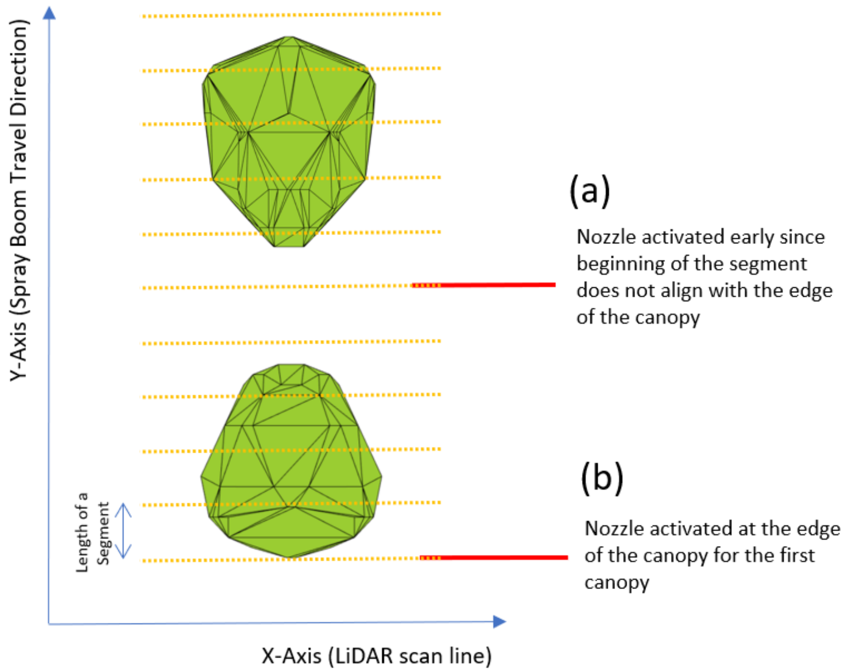

Figure 3-10: The nozzle activation error is associated with the spatial resolution of the laser scan. The maximum error is the length of a segment. (a) shows early nozzle activation where the dataset is split (red line in the figure), does not intercept with the plant canopy. (b) shows zero nozzle activation error where the dataset is split, is tangent to the plant canopy. The yellow lines depict the locations of where the laser dataset is split into segments.

3.4.1.2 Nozzle Alignment

Since there are many nozzles on a given spray boom, it is essential to assure all nozzles are activated accurately whether they are close or far from the LiDAR sensor. Figure 3-11 shows the nozzle activation errors for objects at different distances from the laser sensor. The system in the greenhouse travelled at a speed of 0.224 m/s; hence, the acceptable error threshold was 28 mm (Equation 3.8). The nozzles were activated before the edges of the objects for all observations. When the objects were placed 1.5 m from the laser a mean error of 15 mm was observed. Mean errors of 12 mm and 18 mm were observed for objects placed at 2.5 m and 3.5 m from the laser sensor, respectively. The error in laser and nozzle alignment was measured as 1.55˚. This would have resulted in an error of approximately 41, 68, and 95 mm in the nozzle activation at 1.5, 2.5 and 3.5 m from the LiDAR sensor, respectively, if there was no correction for the error. The results from the experiment showed that the increasing distance of the objects from the laser did not result in an increase in error in activation of the nozzles. The laser alignment compensation performed well. The error was also lower than the theoretical error threshold of 28 mm for all distances.

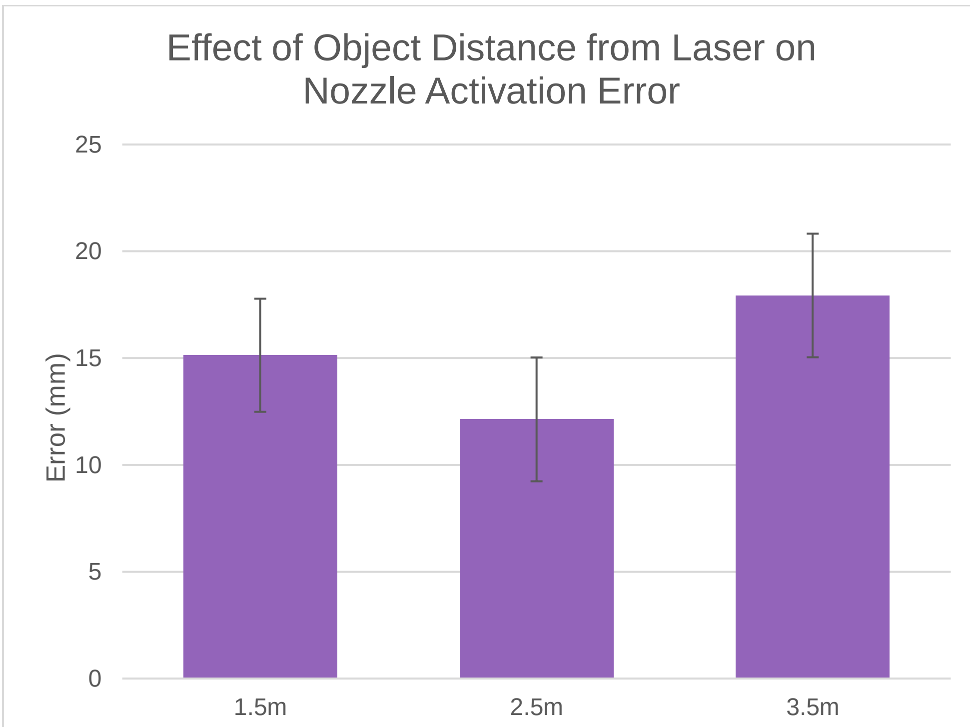

Figure 3-11: The increasing distance of a row of objects from the laser does not have an increasing error in activation. Hence, it can be inferred that the correction in alignment performs well.

3.4.2 Convex Hull Volume Estimation

To evaluate the performance of plant canopy volume estimation, the convex hull approach was compared to the methodology proposed by Yan et al. (2019). The initial evaluation was done in a laboratory environment using artificial targets, including objects of regular geometrical shapes and a group of artificial plants. The methodology was further evaluated in a greenhouse with living plants.

3.4.2.1 Artificial targets

The convex hull approach to canopy volume estimation performed better than the method proposed by Yan et al. (2019) for objects with irregular surfaces and curvatures (Figure 3-12). Mean accuracy was used as a quantitative measure to compare the two methods. The convex hull method had an overall mean accuracy of 82% for all objects compared to 66% using the methodology proposed by Yan et al. (2019). The convex hull method had a mean accuracy of 81% for ’Plant Group-1’ , 83% for the basketballs, and 83% for the toy balls compared to 39%, 58%, and 52%, respectively, using Yan’s methodology (Yan et al., 2019). On the other hand, higher accuracy was obtained using Yan’s approach for boxes and cylinders, with a mean accuracy of 93% and 86%, respectively, than that achieved by the convex hull approach, with mean accuracies of 80% and 81%, respectively. The shape of the target objects had an impact on the performance of both methodologies. Yan et al. (2019), as mentioned earlier, assumes each point in the dataset to be a bar with unit length and width whose height is determined by the distance of the point from the ground. The volume is calculated as the cumulative volume of these bars; hence, it estimates objects with uniform cross section, such as the boxes and cylinders better than objects that have irregular cross sections like ‘Plant Group-1’, the toy balls, and basketballs. The convex hull method on the other hand follows the contours of target objects to estimate volumes. Plant canopies are irregular in shape; therefore, the convex hull method is better suited for plant volume estimation applications.

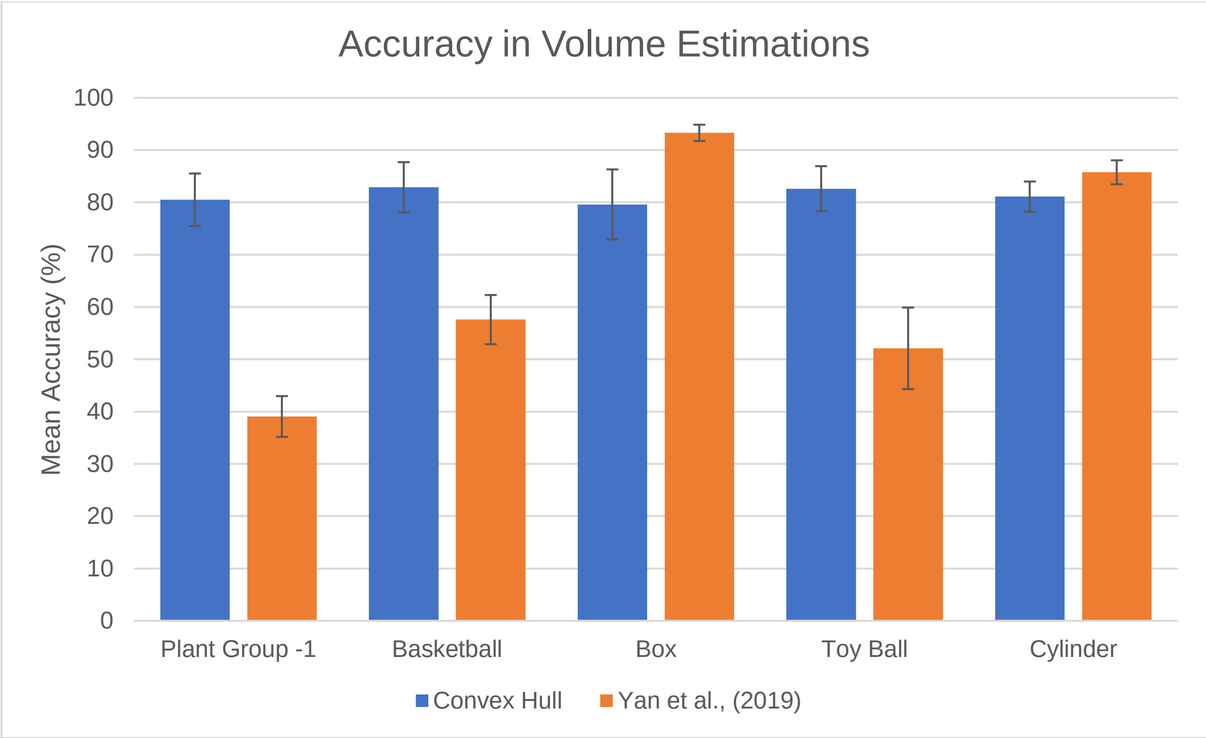

Figure 3-12: The comparison in performance of volume calculations between Yan et al. (2019) and the convex hull approach. The convex hull approach performs better for objects with irregular surfaces and curves, which are more representative of plant canopy shapes

3.4.2.2 Living plants

The performance of the algorithm was further evaluated against manually measured plant canopy volumes in a greenhouse environment with three different sizes of plant canopies (Table 3-4). The convex hull method had a mean accuracy of 83%. Five plants were manually measured in each size of plant canopy. The convex hull method achieved the lowest mean accuracy of 72% with a large standard deviation for the big canopies. The medium sized canopy volumes were estimated with an accuracy of 95%, while accuracy of the small canopy volume measurements was 82%. The algorithm tended to overestimate the volumes of canopies placed within 1 m of the laser sensor (Chapter 2). This effect was more pronounced for the big canopies.

Table 3-4: The performance of the convex hull approach in estimating canopy volumes in a greenhouse environment. A mean overall accuracy of 82.89% was achieved. The standard deviations are in parenthesis.

Target	Mean Accuracy (%)
Big Canopies	72 (20)
Medium Canopies	95 (6)
Small Canopies	82 (10)

3.4.3 Spray Volume Laboratory Evaluation

The spray volume measured was consistently lower for the convex hull approach over all nozzles compared to that of Yan's approach (Yan et al., 2019). Table 3-5 shows the mean measured volumes, calculated volumes based on the duty cycle data sent to the nozzles, and the savings. A mean spray volume reduction of approximately 15% was observed over all nozzles and all canopy sizes. The measured spray volume was higher than the calculated spray volumes (Equation 3.7) for both methodologies. This was due to the physical limitation of the PWM solenoid valves not closing at the right time since the duty cycles are changed every 0.125 s (Yan et al.,2019) plus an excess dribble when the nozzles were turned off. The excess measured volumes also resulted in lower measured spray savings compared to the calculated/potential spray savings.

Table 3-5: The spray volume outputs of the two methods - convex hull and Yan et al. (2019) are compared. The average volumes shown are those of the outputs of seven nozzles for three different sizes of artificial plant canopies. The convex hull approach consistently showed lower spray volumes and achieved an average saving of 15%. Standard deviations are in parenthesis.

Target	Parameters	Convex Hull	Yan et al. (2019)
Plant Group-1	Mean Measured Vol (ml)	5.88 (0.92)	6.81 (0.93)
	Calculated Vol (ml)	2.19	2.84
	Measured spray savings	14%	
	Potential savings	23%	
Plant Group-2	Mean Measured Vol (ml)	3.24 (0.36)	4.01 (0.36)
	Calculated Vol (ml)	1.14	1.46
	Measured spray savings	19%	
	Potential savings	22%	
Plant Group-3	Mean Measured Vol (ml)	9.08 (0.78)	10.28 (0.64)
	Calculated Vol (ml)	2.95	3.95
	Measured spray savings	12%	
	Potential savings	25%	

The three groups of artificial plants resulted in three different spray volume outputs, which shows that the variable-rate spray system functioned effectively. ‘Plant Group-3’ had the highest average spray volume output of 9.08 ml for the convex hull method while Yan et al. (2019) was 10.28 ml. ‘Plant Group-1’ had mean spray volumes of 5.88 ml and 6.81 ml for the convex hull method and Yan et al. (2019), respectively. ‘Plant Group-2’ resulted in 3.24 ml and 4.01 ml mean spray volumes for the convex hull and Yan et al. (2019) methods, respectively. ‘Plant Group-2’ showed the greatest reduction in spray volume at 19%. This might not be the best measure since a few of the duty cycles for the small canopies were below 20%, where the spray nozzle performance is not reliable (Gu et al., 2011). ‘Plant Group-1’ showed 14% and ‘Plant Group-3’ showed 12% spray savings. The consistent reduction in volume between the two methods shows that the improvement in volume estimation results in greater spray volume savings.

3.4.4 Spray Coverage

A deposition study was conducted in a production greenhouse to evaluate the offline spraying system's performance for pest management based on its effectiveness and efficiency. For the effectiveness of insecticides, herbicides and fungicides, a coverage of at least 30% is required for disease prevention. If coverage is less than 30%, a droplet density of 20-30 droplets/cm^2 is sufficient for insecticides and 50-70 droplets/cm^2 is sufficient for fungicides (Zhu et al., 2011).

The spray coverage performance of three different spraying strategies was evaluated using deposition data collected with WSP targets located at three different locations in the plant canopy (Section 3.3.3). Table 3-6, Table 3-7, and Table 3-8 show the percentage coverage obtained by the three strategies at the edges, including leading edge and trailing edge of a plant canopy; bottom; and top of the plant canopies, respectively. C1, C2, … C16 are plant locations where the WSP targets were placed as shown in Figure 3-8(a).

Table 3-6 shows that the offline system significantly reduced the spray coverage on the edges of plant canopies compared to the other two systems. This shows that the offline system improved on the overestimation of edge canopy densities of the Yan et al. (2019) system and a precise spray rate control for intra-canopy density variations was achieved. The algorithm significantly reduced spray coverage for canopies placed beyond 3.5 m from the laser sensor (C1, C5, and C9), which shows that the offline system with the use of the newly developed processing algorithm was able to better characterize plant canopies further from the laser. The offline system had a spray coverage well above the recommended 30% for all canopies except C9. The mean spray coverage for C9 was 28.57% and the mean droplet density was 58.6 droplets/cm^2, with a standard deviation of 21.7 droplets/cm^2. This droplet density would have been sufficient for insecticides and herbicides but not for fungicides. C9 was a small canopy placed at around 4 m from the laser sensor. The dimensions of the canopy were underestimated due to the reduction in resolution of the laser dataset as the distance from the laser increased. This resulted in less than ideal spray volume output.

Table 3-6: The percentage coverage for the WSP placed at the edges of the plant canopies. Three repetitions were performed for each method and two edges were measured for each canopy, resulting in a total sample size of 6. Standard deviations are in parenthesis. Same letters within the same column and same canopy show there is no significant difference (α=0.05). C1, C3, C5, C7, C9, and C11 are the labels provided for selected plant canopies that had WSP placed at their edges.

Deposition Target – Canopy - Edges				
Method	C1	C3	C5	C7
Yan et al. (2019)	92.87 (5.57) a	99.58 (0.23) a	96.9 (3.68) a	98.19 (2.65) a
Offline	79.59 (5.07) b	97.74 (0.95) b	84.68 (5.93) b	90.60 (4.23) b
Conventional	97.82 (0.93) a	99.72 (0.25) a	99.01 (1.33) a	99.93 (0.06) a
	C9	C11		
Yan et al. (2019)	96.22 (2.04) a	74.11 (9.88) b		
Offline	28.57 (7.32) c	85.42 (6.89) b		
Conventional	81.58 (8.56) b	99.67 (0.35) a		

Table 3-7 shows that there was no significant difference between the spray coverage achieved by the offline system and the Yan et al. (2019) system at the bottom of most plant canopies; Thus, the lower spray rates of the offline system still managed to penetrate the plant canopies effectively. There was no significant difference for the canopies placed in tightly packed blocks (C2, C4, C6, and C8). The offline system spray coverage was significantly lower than the Yan et al. (2019) system for canopies C14 and C15 that were in sparsely populated blocks. The reduction in spray coverage was below the recommended 30% for the offline system in canopies C4, C13, C14, C15 and C16. The droplet densities for the respective canopies were 134.76 (39), 106.37 (66), 110.87 (15.5), 58.37 (33.12), 80.67 (4.35) droplets/cm^2. From the density and coverage data, it can be inferred that only C15 had a lower than recommended spray coverage and density for fungicides, yet it was sufficient for insecticides and herbicides. The spray coverage can be improved by using nozzles that have a greater flow rate to penetrate the canopies better; However, it may increase the total spray volume used and result in over-spraying of the rest of the plant canopy.

Table 3-7: The percentage cover for the WSP placed at the bottom of the plant canopies. Three repetitions were performed for each method for each plant canopy. Standard deviations are in parenthesis. Same letters within the same column and same canopy show there is no significant difference (α=0.05)*. C2, C4, C6, C8, C13, C14, C15, and C16 are the labels provided for select plant canopies that had WSP placed the bottom of the canopy.*

Deposition Target – Canopy – Bottom				
Method	C2	C4	C6	C8
Yan et al. (2019)	28.16 (5.75) a	16.02 (6.81) a	29.88 (19.25) a	33.56 (33.86) a
Offline	28.69 (2.88) a	13.29 (2.98) a	30.71 (28.69) a	32.76 (9.45) a
Conventional	31.22 (2.86) a	23.09 (5.97) a	79.66 (7.55) a	78.50 (2.80) a
	C13	C14	C15	C16
Yan et al. (2019)	17.89 (10.57) b	49.42 (11.26) b	27.6 (5.10) b	21.98 (19.6) b
Offline	11.02 (3.69) b	21.31 (5.52) c	7.27 (3.80) c	17.12 (7.83) b
Conventional	68.70 (11.96) a	79.89 (11.17) a	38.58 (2.82) a	85.21 (0.04) a

The offline system showed a significant reduction in spray coverage while maintaining values well above the recommended 30% at the top of plant canopies (Table 3-8). The spray coverage achieved by the offline system was significantly lower than the Yan et al. (2019) system for C10, C13, C14, and C15. It was also significantly lower than the conventional system for all canopies except C2, C4 and C12. These results show that the offline system managed to reduce over-spraying at the tops of canopies.

Table 3-8: The percentage coverage for the WSP placed at the top of the plant canopies. Three repetitions were performed for each method and for each canopy. Standard deviations are in parenthesis. Same letters within the same column and same canopy show there is no significant difference (α=0.05). *C2, C4, C6, C8, C10, C12, C13, C14, C15, and C16 are the labels provided for select plant canopies that had WSP placed the top of the canopy.*

Deposition Target – Canopy - Top				
Method	C2	C4	C6	C8
Yan et al. (2019)	98.91 (0.71) a	99.45 (0.29) b	97.61 (3.02) ab	95.02 (3.20) ab
Offline	93.09 (4.51) a	99.90 (0.05) a	84.34 (8.68) b	95.12 (1.25) b
Conventional	99.25 (0.09) a	99.91 (0) a	99.87 (0.04) a	99.87 (0.04) a
	C10	C12	C13	C14
Yan et al. (2019)	97.38 (0.70) a	42.93 (14.10) b	99.91 (0.11) a	99.65 (0.36) a
Offline	93.48 (2.47) b	93.78 (1.46) a	82.85 (2.88) b	85.94 (1.03) b
Conventional	99.61 (0.24) a	99.79 (0.29) a	99.96 (0.02) a	99.95 (0.02) a
	C15	C16		
Yan et al. (2019)	99.57 (0.72) a	84.05 (1.02) b		
Offline	87.64 (3.73) b	82.97 (3.98) b		
Conventional	99.8 (0.13) a	99.8 (0.13) a		

The spray coverage on the ground targets were significantly lower than the conventional for both variable-rate spray systems, which shows there was a reduced loss of spray to the ground (Table 3-9). The offline system also had significantly lower spray coverage than that of the Yan et al. (2019) system on the ground targets G1, G3, G5 and G9. This finding indicates that the offline system was able to reduce off-target losses further. The targets G2, G4, and G6, placed behind the trailing edges of the plant canopies had higher coverage percentages than G1, G3, and G5, placed ahead of the leading edges of plant canopies. This may have been due to a slight spray drift inside the greenhouse along the travel direction of the spray boom. There was also no significant difference in spray coverage between the Yan et al. (2019) system and the offline system for G2, G4, and G6. This may have been because the Yan et al. (2019) system did not account for the error in laser alignment resulting in the nozzles being turned off earlier than intended. G7 had the highest spray coverage for both the Yan et al. (2019) system as well as the offline system, which due to the WSP being within the range of the nozzles that were activated.

G8 and G10 showed minimal coverage for both variable-rate spray systems, while there was a significant reduction between the two variable-rate systems for G9. The conventional system predictably achieved a 100% spray coverage on the ground targets showing their large off-target losses.

Table 3-9: Percentage coverage for the WSP placed on the ground. Three repetitions were performed for each method and for each canopy. Standard deviations are in parenthesis. Same letters within the same column and same canopy show there is no significant difference (α=0.05). *G1, G2 … G10 are the labels provided for select ground targets.*

Deposition Target - Ground				
Method	G1	G2	G3	G4
Yan et al. (2019)	83.59 (10.87) a	46.44 (3.16) b	72.41 (7.70) b	49.91 (16.18) b
Offline	6.71 (5.53) b	39.55 (8.69) b	13.27 (1.18) c	26.42 (4.32) b
Conventional	100 (0) a	100 (0) a	100 (0) a	100 (0) a
	G5	G6	G7	G8
Yan et al. (2019)	6.54 (3.40) b	52.65 (33.51) a	33.04 (13.31) b	0.19 (0.24) b
Offline	0.35 (0.12) c	80.26 (0.48) a	16.91 (6.25) b	0.56 (0.63) b
Conventional	100 (0) a	100 (0) a	99.95 (0.08) a	100 (0) a
	G9	G10		
Yan et al. (2019)	11.31 (3.26) b	0.51 (0.49) b		
Offline	3.37 (0.95) c	0.34 (0.24) b		
Conventional	100 (0) a	100 (0) a		

The variable-rate spraying systems showed a significant reduction in spray volume used compared to the conventional, constant spray system. The total spray volume used by the Yan et al. (2019) system was 5.06 liters. The offline system used 2.36 liters while the conventional system used 16.43 liters. There was a reduction of 86% with the offline system compared to the conventional spray system. The offline system achieved a 53% reduction in spray volume used compared to Yan et al. (2019) while maintaining spray coverage and droplet density above the recommended values for all canopies. These results show that the offline system was able to improve the efficiency of the existing variable-rate sprayer by 53%, using precise intra-canopy spray rate variations and reduced losses to the ground.

3.5 APPLICATIONS AND IMPROVEMENTS

The convex hull approach with the processing algorithm could be integrated into the system while maintaining inline operation if the computing power of the system can be improved. This integrated inline system could improve spray efficiencies while eliminating potential increases in operational costs due to running the system multiple times. The methodology used to correct for the laser alignment can also reduce off-target losses and result in better spray coverage of plant canopies.

Offline functionality, on the other hand, can provide further flexibility in how the laser data is collected. The current system, which has one laser sensor for each spray boom, may not be economically feasible when considering the large number of spray booms in a commercial greenhouse. Hence, mapping the whole greenhouse through more cost-effective methods such as utilizing an UAV (Unmanned Aerial Vehicle) while spraying offline could potentially lead to significant reductions in system costs.

3.6 CONCLUSIONS

The accommodation of an improved canopy characterization algorithm required the modification of an inline system (Yan et al., 2019) to an offline system. This study focused on two aspects of spray control: spray location and spray volume control. The developed methodologies were tested both in a laboratory and a commercial greenhouse. As a result, the offline system achieved 53% and 86% spray volume reductions compared to an intelligent greenhouse sprayer developed by Yan et al. (2019) and a conventional spray system, respectively.

For the spray location control, the algorithm developed was found effective in detecting and initiating a sequence of spray operations. For precise spraying location of all nozzles on a spray boom, it was aligned with the LiDAR/laser sensor that was used to collect plant information. The nozzles were found to activate within a mean distance of 7 mm from the edge of the plant canopies. The distance travelled by the nozzles did not show any effect on the timing of activation.

Improved canopy volume determination was possible using a convex hull approach and was shown to improve volume estimations compared to that by Yan et al. (2019) for objects with irregular surfaces and curvatures, which are more representative of plant canopy shapes. It achieved a mean accuracy of 82% compared to 66% for the methodology reported by Yan et al. (2019). The improvement in volume measurements also showed an improvement in spray volume outputs with an average reduction of 15% in spray volume based on laboratory tests.

It was further found that the intra-canopy precision control, according to varied canopy density, resulted in improved spray efficiency while meeting most of the coverage requirements. The spray coverage evaluation was conducted in a commercial production greenhouse. The improved efficiency was due to a significant reduction in spray coverage at the edges of plant canopies that have lower canopy density, while staying above recommended spray coverage percentages. At the center, where the density is the highest, the tops and bottoms of the canopies achieved similar coverage as the Yan et al. (2019) system and the conventional system for plant canopies that were grouped closely together. It significantly reduced off-target losses as seen from the spray coverage data of the ground targets. The coverage was reduced to below recommended values for the offline system in the bottoms of a few plant canopies. The low spray coverage still had a density of droplets which was sufficient for pest prevention.

Chapter 4: Conclusions and Recommendations for Future Study

The efficiency of a 2D laser-guided, variable rate sprayer (Yan et al., 2019) was improved by reducing spray volume use by 53% in a greenhouse environment. This reduction in spray volume was achieved through the introduction of a processing algorithm (CHBC) that improved canopy characterization. CHBC involved the use of a combination of registration algorithm, clustering algorithm and a mirroring algorithm. The improvement was measured using a root mean square error (RMSE) parameter. The RMSE in canopy width measurements – the major shortcoming of Yan et al., (2018) was reduced by 46% when using CHBC. CHBC achieved an average RMSE of 25 mm compared to Yan et al., (2018) which was 47 mm when the laser sensor was placed at a height of 1 m. Greater laser sensor heights reduced RMSE for both the Yan et al. (2018) methodology as well as CHBC but the latter methodology was more accurate and robust at different sensor heights. CHBC also performed more reliably for plants placed at increasing horizontal distances from the sensor when the sensor height was determined by calculating an 'optimal sensor height' whose formula was derived using principles developed by Sun et al. (2017).

The inline variable rate spray system developed by Yan et al., (2019) was modified to incorporate the CHBC algorithm. The computing time required by the CHBC algorithm meant that the system could no longer have inline functionality. The system was converted to operate offline and split its functions into a two-step process. It was made to perform one run where the plant canopies were scanned and spray on a second run. A new GUI was designed to facilitate this two-step process. The location of when the nozzles were activated for the spray run was determined by detecting the presence of the plant canopies using the data recorded from the previous scan run. A similarity index was used to compare the laser data obtained during the spray run to the data obtained from the scan run. When the two datasets matched, it meant that the plant canopies were located. The performance of this detection algorithm was tested by locating where the nozzles were activated. It was found to activate within 7.23 mm of the edges of the plant canopies.

The spray rates were calculated offline using the CHBC processed data. They were calculated as a function of the volume of the plant canopies. A convex hull was used to calculate volumes and increased the accuracy compared to the Yan et al., (2019) methodology. A mean accuracy of 81% was achieved by the convex hull compared to 66% of Yan et al., (2019). A reduction of 15% in spray volume was also observed in a lab environment when using the convex hull method which was able to precisely control spray rates based on intra-canopy variations in density. The offline system using the CHBC processed data and the convex hull to calculate volumes was tested in a greenhouse environment. Its spray coverage over plant canopies was compared to the Yan et al., (2019) system as well a conventional system. No significant difference in spray coverage was observed for the top and bottom of plant canopies grouped close together. The edges of the canopies sprayed by the offline system showed a significant reduction in spray coverage while staying above recommended values. There was also a significant reduction in off-target losses. The bottom of plant canopies placed in sparse rows showed a reduction in spray coverage below recommended values, but the density of spray was still sufficient for disease prevention using insecticides and herbicides but not for fungicides. The offline system reduced spray volumes by 87% compared to the conventional system and improved the efficiency of the Yan et al., (2019) system by 53%.

The algorithm developed in this study can be further developed to resolve some limitations. The ground datapoints interfere with the CHBC algorithm and are removed currently by manually measuring the height of the sensor from the ground and inputting the value into the program. This can be automated in the future.

The computing time can also be reduced through further improvement of the code. The test area of the greenhouse was restricted to about 16m in length and the CHBC algorithm took about 15 min to process close to 2.5 million datapoints.

The mirroring algorithm assumes plant canopies are symmetrical and this may not be the best assumption since it overestimates the canopy dimensions for plants closer to the laser. Hence further studies can be performed to develop better ways to predict the occluded sides of the plant canopies.

The offline spray system can also be improved further for commercial use inside a greenhouse. The current system obtains laser data from the GUI but processes it separately on a numerical computing platform. The processed data is then fed back to the GUI to spray the canopies. A more cohesive single platform data collection and processing is desirable. The spray efficiency can also be improved further by studying the effect of the overlapping spray coverage areas between adjacent nozzles.

Bibliography

Auat Cheein, F. A., Guivant, J., Sanz, R., Escolà, A., Yandún, F., Torres-Torriti, M., Rosell-Polo, J. R. (2015). Real-time approaches for characterization of fully and partially scanned canopies in groves. *Computers and Electronics in Agriculture*, *118*, 361–371. https://doi.org/10.1016/j.compag.2015.09.017

Berenstein, R., Shahar, O. B., Shapiro, A., Edan, Y. (2010). Grape clusters and foliage detection algorithms for autonomous selective vineyard sprayer. *Intelligent Service Robotics*, *3*(4), 233–243. https://doi.org/10.1007/s11370-010-0078-z

Besl, P. J., McKay, N. D. (1992). A method for registration of 3-D shapes. *IEEE Transactions on Pattern Analysis and Machine Intelligence*, *14*(2), 239–256. https://doi.org/10.1109/34.121791

Bosnak, M. (2017). Evolving principal component clustering for 2-D LIDAR data. In *2017 Evolving and Adaptive Intelligent Systems (EAIS)* (pp. 1–6). Ljubljana, Slovenia: IEEE. https://doi.org/10.1109/EAIS.2017.7954834

Braekman, P., Foqué, D., Labeke, M.-C. V., Pieters, J. G., Nuyttens, D. (2009). Influence of Spray Application Technique on Spray Deposition in Greenhouse Ivy Pot Plants Grown on Hanging Shelves. *HortScience*, *44*(7), 1921–1927. https://doi.org/10.21273/HORTSCI.44.7.1921

Bulyshev, A. (2014). A Super-Resolution Algorithm for Enhancement of FLASH LIDAR Data: Flight Test Results. Presented at the SPIE Electronic Imaging, San Francisco, CA, United States. Retrieved from https://ntrs.nasa.gov/search.jsp?R=20140011915

Çayir, A., Coskun, M., Coskun, M., Cobanoglu, H. (2018). DNA damage and circulating cell free DNA in greenhouse workers exposed to pesticides. *Environmental and Molecular Mutagenesis*, *59*(2), 161–169. https://doi.org/10.1002/em.22148

Cayir, A., Coskun, M., Coskun, M., Cobanoglu, H. (2019). Comet assay for assessment of DNA damage in greenhouse workers exposed to pesticides. *Biomarkers*, *24*(6), 592–599. https://doi.org/10.1080/1354750X.2019.1610498

Chakraborty, M., Khot, L. R., Sankaran, S., Jacoby, P. W. (2019). Evaluation of mobile 3D light detection and ranging based canopy mapping system for tree fruit crops. *Computers and Electronics in Agriculture*, *158*, 284–293. https://doi.org/10.1016/j.compag.2019.02.012

Chen, Y., Zhu, H., Ozkan.H. E. (2012). Development of a Variable-Rate Sprayer with Laser Scanning Sensor to Synchronize Spray Outputs to Tree Structures. *Transactions of the ASABE*, *55*(3), 773–781. https://doi.org/10.13031/2013.41509

Chen, Y., Zhu, H., Ozkan. H. E. (2013). Real-time Tree Foliage Density Estimation with Laser Scanning Sensor for Variable-Rate Tree Sprayer Development. In *2013 Kansas City, Missouri, July 21 - July 24, 2013*. American Society of Agricultural and Biological Engineers. https://doi.org/10.13031/aim.20131596009

Chen, Y., Zhu, H., Ozkan, H. E. (2013) Spray Deposition inside Tree Canopies from a Newly Developed Variable-Rate Air-Assisted Sprayer. Transactions of the ASABE. 56(6): 1263-1272. (doi: 10.13031/trans.56.9839) @2013

Damalas, C. A., Eleftherohorinos, I. G. (2011). Pesticide Exposure, Safety Issues, and Risk Assessment Indicators. *International Journal of Environmental Research and Public Health*, *8*(5), 1402–1419. https://doi.org/10.3390/ijerph8051402

Derksen, R. C., Ranger, C. M., Cañas, L. A., Locke, J. C., Zhu, H., Krause, C. R. (2010). Evaluation of Handgun and Broadcast Systems for Spray Deposition in Greenhouse Poinsettia Canopies. *Transactions of the ASABE*, *53*(1), 5–12. https://doi.org/10.13031/2013.29494

Derksen, R. C., Frantz, J.; Ranger, C. M., Locke, J. C., Zhu, H., Krause., C. R. (2008). Comparing Greenhouse Handgun Delivery to Poinsettias by Spray Volume and Quality. *Transactions of the ASABE*, *51*(1), 27–35. https://doi.org/10.13031/2013.24214

Del Prado-Lu, J. L. (2007). Pesticide exposure, risk factors and health problems among cutflower farmers: a cross sectional study. *Journal of Occupational Medicine and Toxicology*, *2*(1), 9. https://doi.org/10.1186/1745-6673-2-9

Escolà, A. (2010, June 10). *Method for real-time variable rate application of plant protection products in precision horticulture/fructiculture at http://hdl.handle.net/10803/8158*.

Escolà, A., Martínez-Casasnovas, J. A., Rufat, J., Arnó, J., Arbonés, A., Sebé, F., … Rosell-Polo, J. R. (2017). Mobile terrestrial laser scanner applications in precision fruticulture/horticulture and tools to extract information from canopy point clouds. *Precision Agriculture*, *18*(1), 111–132. https://doi.org/10.1007/s11119-016-9474-5

Ester, M., Kriegel, H.-P., Sander, J., Xu, X. (1996). A density-based algorithm for discovering clusters in large spatial databases with noise. In *Proceedings of the Second International Conference on Knowledge Discovery and Data Mining* (pp. 226–231). Portland, Oregon: AAAI Press.

Gené-Mola, J., Gregorio, E., Auat Cheein, F., Guevara, J., Llorens, J., Sanz-Cortiella, R., … Rosell-Polo, J. R. (2020). Fruit detection, yield prediction and canopy geometric characterization using LiDAR with forced air flow. *Computers and Electronics in Agriculture*, *168*. https://doi.org/10.1016/j.compag.2019.105121

Ghosh, S., Lohani, B. (2013). Mining lidar data with spatial clustering algorithms. *International Journal of Remote Sensing*, *34*(14), 5119–5135. https://doi.org/10.1080/01431161.2013.787499

Gil, E., Escolà, A., Rosell, J. R., Planas, S., Val, L. (2007). Variable rate application of plant protection products in vineyard using ultrasonic sensors. *Crop Protection*, *26*(8), 1287–1297. https://doi.org/10.1016/j.cropro.2006.11.003

Giles, D. K., Klassen, P., Niederholzer, F. J. A., Downey, D. (2011). "Smart" sprayer technology provides environmental and economic benefits in California orchards. *California Agriculture*, *65*(2), 85–89.

Glasner, D., Bagon, S., Irani, M. (2009). Super-resolution from a single image. In *2009 IEEE 12th International Conference on Computer Vision* (pp. 349–356). Kyoto: IEEE. https://doi.org/10.1109/ICCV.2009.5459271

Goossens, E., Windey, S., Sonck, B. (2004). Information service and voluntary testing of spray guns and other types of sprayers in horticulture. *Asp. Appl. Biol.*, *71*.

Gu, J., Zhu, H., Ding, W., Jeon, H. Y. (2011). DROPLET SIZE DISTRIBUTIONS OF ADJUVANT-AMENDED SPRAYS FROM AN AIR-ASSISTED FIVE-PORT PWM NOZZLE. *Atomization and Sprays*, *21*(3). https://doi.org/10.1615/AtomizSpr.2011003258

Guo, Y., Sohel, F., Bennamoun, M., Wan, J., Lu, M. (2014). An Accurate and Robust Range Image Registration Algorithm for 3D Object Modeling. *IEEE Transactions on Multimedia*, *16*(5), 1377–1390. https://doi.org/10.1109/TMM.2014.2316145

Haarstad, K., Bavor, J., Roseth, R. (2012). Pesticides in Greenhouse Runoff, Soil and Plants: A Screening. *The Open Environmental & Biological Monitoring Journal*, *5*(1). Retrieved from https://benthamopen.com/ABSTRACT/TOEBMJ-5-1

Heun, J. T., Attalah, S., French, A. N., Lehner, K. R., McKay, J. K., Mullen, J. L., … Andrade-Sanchez, P. (2019). Deployment of lidar from a ground platform: Customizing a low-cost, information-rich and user-friendly application for field phenomics research. *Sensors (Switzerland)*, *19*(24). https://doi.org/10.3390/s19245358

Hornacek, M., Rhemann, C., Gelautz, M., Rother, C. (2013). Depth Super Resolution by Rigid Body Self-Similarity in 3D. In *2013 IEEE Conference on Computer Vision and Pattern Recognition* (pp. 1123–1130). Portland, OR, USA: IEEE. https://doi.org/10.1109/CVPR.2013.149

Jain, A. K., Murty, M. N., Flynn, P. J. (1999, September 1). Data clustering: a review. Association for Computing Machinery. Retrieved from https://doi.org/10.1145/331499.331504

Jenkins, E., Hines, R. (2003). Chapter 4: Spraying fruit. *Fruit crop pest management. A guide for commercial applicators category 1C.* Michigan St. Univ. 124pp.

Jeon, H. Y., Zhu, H. (2012). Development of a Variable-Rate Sprayer for Nursery Liner Applications. *Transactions of the ASABE*, *55*(1), 303–312. https://doi.org/10.13031/2013.41240

Kil, Y. J., Amenta, N., Mederos, B. (2006). Laser Scanner Super-resolution. Retrieved from https://escholarship.org/uc/item/4vr5f59d

Lee, K. H., Ehsani. R. (2009). A Laser Scanner Based Measurement System for Quantification of Citrus Tree Geometric Characteristics. *Applied Engineering in Agriculture*, *25*(5), 777–788. https://doi.org/10.13031/2013.28846

Li, W., Guo, Q., Jakubowski, M. K., Kelly, M. (2012). A New Method for Segmenting Individual Trees from the Lidar Point Cloud. *Photogrammetric Engineering & Remote Sensing*, *78*(1), 75–84. https://doi.org/10.14358/PERS.78.1.75

Liu, P., Zhou, D., Wu, N. (2007). VDBSCAN: Varied Density Based Spatial Clustering of Applications with Noise. In *2007 International Conference on Service Systems and Service Management* (pp. 1–4). https://doi.org/10.1109/ICSSSM.2007.4280175

Liu, H., Zhu, H., Shen, Y. (2014). Development of Digital Flow Control System for Multi Channel Variable-Rate Sprayers. Transactions of the ASABE. 57(1): 273-281. (doi:10.13031/trans.57.10216) @2014

Liu, H., Zhu, H. (2016). Evaluation of a laser scanning sensor in detection of complex-shaped targets for variable-rate sprayer development. *Trans. ASABE, 59*(5), 1181-1192.

Llop, J., Gil, E., Llorens, J., Miranda-Fuentes, A., Gallart, M. (2016). Testing the Suitability of a Terrestrial 2D LiDAR Scanner for Canopy Characterization of Greenhouse Tomato Crops. *Sensors*, *16*(9), 1435. https://doi.org/10.3390/s16091435

Llorens, J., Gil, E., Llop, J., Escolà, A. (2011). Ultrasonic and LIDAR Sensors for Electronic Canopy Characterization in Vineyards: Advances to Improve Pesticide Application Methods. *Sensors*, *11*(2), 2177–2194. https://doi.org/10.3390/s110202177

Mac Aodha, O., Campbell, N. D. F., Nair, A., Brostow, G. J. (2012). Patch Based Synthesis for Single Depth Image Super-Resolution. In A. Fitzgibbon, S. Lazebnik, P. Perona, Y. Sato,

& C. Schmid (Eds.), *Computer Vision – ECCV 2012* (Vol. 7574, pp. 71–84). Berlin, Heidelberg: Springer Berlin Heidelberg. https://doi.org/10.1007/978-3-642-33712-3_6

Mitra, N. J., Gelfand, N., Pottmann, H., Guibas, L. (2004). Registration of point cloud data from a geometric optimization perspective. In *Proceedings of the 2004 Eurographics/ACM SIGGRAPH symposium on Geometry processing - SGP '04* (p. 22). Nice, France: ACM Press. https://doi.org/10.1145/1057432.1057435

Nyström Johansson, T., Wellenstam, O. (2017). *LiDAR clustering and shape extraction for automotive applications* (Master's Thesis).

Osman, K. A., Al-Humaid, A. I., Al-Rehiayani, S. M., Al-Redhaiman, K. N. (2011). Estimated daily intake of pesticide residues exposure by vegetables grown in greenhouses in Al-Qassim region, Saudi Arabia. *Food Control*, *22*(6), 947–953. https://doi.org/10.1016/j.foodcont.2010.11.031

Pergher, G., Gubiani, R., Tonetto, G. (1997). Foliar deposition and pesticide losses from three air-assisted sprayers in a hedgerow vineyard. *Crop Protection*, *16*(1), 25–33. https://doi.org/10.1016/S0261-2194(96)00054-3

Reiser, D., Vázquez-Arellano, M., Paraforos, D. S., Garrido-Izard, M., Griepentrog, H. W. (2018). Iterative individual plant clustering in maize with assembled 2D LiDAR data. *Computers in Industry*, *99*, 42–52. https://doi.org/10.1016/j.compind.2018.03.023

Roseth, R., Haarstad, K. (2010). Pesticide runoff from greenhouse production. *Water Science and Technology*, *61*(6), 1373–1381. https://doi.org/10.2166/wst.2010.040

Salyani, M., Heping Zhu, Sweeb, R. D., Pai, N. (2013). Assessment of spray distribution with water-sensitive paper. *Agricultural Engineering International: CIGR Journal*, *15*(2), 101–111.

Sánchez-Hermosilla, J., Páez, F., Rincón, V. J., Pérez-Alonso, J. (2013). Volume application rate adapted to the canopy size in greenhouse tomato crops. *Scientia Agricola*, *70*(6), 390–396. https://doi.org/10.1590/S0103-90162013000600003

Sánchez-Hermosilla, J., Rincón, V. J., Páez, F., Agüera, F., Carvajal, F. (2011). Field evaluation of a self-propelled sprayer and effects of the application rate on spray deposition and losses to the ground in greenhouse tomato crops. *Pest Management Science*, *67*(8), 942–947. https://doi.org/10.1002/ps.2135

Satnam Singh, Thomas Burks, W S Lee. (2004). AUTONOMOUS Robotic Vehicle for Greenhouse Spraying. In *2004, Ottawa, Canada August 1 - 4, 2004*. American Society of Agricultural and Biological Engineers. https://doi.org/10.13031/2013.16729

Shen, Y., Zhu, H., Liu, H., Chen, Y., Ozkan, E. (2017). Development of a laser-guided, embedded-computer-controlled, air-assisted precision sprayer. *Trans. ASABE.* *60*(6),1827-1838.

Seiber, J. N., Wilson, B. W., McChesney, M. M. (1993). Air and fog deposition residues of four organophosphate insecticides used on dormant orchards in the San Joaquin Valley, California. *Environmental Science & Technology*, *27*(10), 2236–2243. https://doi.org/10.1021/es00047a034

Semchuk, K. M., Love, E. J., Lee, R. G. (1992). Parkinson's disease and exposure to agricultural work and pesticide chemicals. *Neurology*, *42*(7), 1328. https://doi.org/10.1212/WNL.42.7.1328

Shen, Y., Zhu, H., Liu, H., Chen, Y., Ozkan, E. (2017). Development of a Laser-Guided, Embedded-Computer-Controlled, Air-Assisted Precision Sprayer. *Transactions of the ASABE*, *60*(6), 1827–1838. https://doi.org/10.13031/trans.12455

Siebers, J., Mattusch, P. (1996). Determination of airborne residues in greenhouses after application of pesticides. *Chemosphere*, *33*(8), 1597–1607. https://doi.org/10.1016/0045-6535(96)00279-2

Sinha, R., Ranjan, R., Khot, L. R., Hoheisel, G.-A., Grieshop, M. J. (2020). Comparison of within canopy deposition for a solid set canopy delivery system (SSCDS) and an axial–fan airblast sprayer in a vineyard. *Crop Protection*, *132*, 105124. https://doi.org/10.1016/j.cropro.2020.105124

Spinello, L., Siegwart, R. (2008). Human detection using multimodal and multidimensional features. In *2008 IEEE International Conference on Robotics and Automation* (pp. 3264–3269). https://doi.org/10.1109/ROBOT.2008.4543708

Sun, S., Li, C., Paterson, A. (2017). In-Field High-Throughput Phenotyping of Cotton Plant Height Using LiDAR. *Remote Sensing*, *9*(4), 377. https://doi.org/10.3390/rs9040377

Tsimbiri, P. F., Moturi, W. N., Sawe, J., Henley, P., Bend, J. R. (2015). Health Impact of Pesticides on Residents and Horticultural Workers in the Lake Naivasha Region, Kenya. *Occupational Diseases and Environmental Medicine*, *03*(02), 24. https://doi.org/10.4236/odem.2015.32004

Wang, Y., Weinacker, H., Koch, B. (2008). A Lidar Point Cloud Based Procedure for Vertical Canopy Structure Analysis And 3D Single Tree Modelling in Forest. *Sensors*, *8*(6), 3938–3951. https://doi.org/10.3390/s8063938

Wei, M., Zhao, L., Liu, X. (2014). A new clustering algorithm with adaptive attractor for LIDAR points. In *2014 IEEE International Conference on Progress in Informatics and Computing* (pp. 21–26). Shanghai, China: IEEE. https://doi.org/10.1109/PIC.2014.6972288

Wu, X., Shen, X., Cao, L., Wang, G., Cao, F. (2019). Assessment of Individual Tree Detection and Canopy Cover Estimation using Unmanned Aerial Vehicle based Light Detection and Ranging (UAV-LiDAR) Data in Planted Forests. *Remote Sensing*, *11*(8), 908. https://doi.org/10.3390/rs11080908

Xiao, L., Zhu, H., Wallhead, M., Horst, L., Ling, P., Krause, C. R. (2018). Characterization of Biological Pesticide Deliveries through Hydraulic Nozzles. *Transactions of the ASABE*, *61*(3), 897–908. https://doi.org/10.13031/trans.12698

Yan, T., Zhu, H., Sun, L., Wang, X., Ling, P. (2018). Detection of 3-D objects with a 2-D laser scanning sensor for greenhouse spray applications. *Computers and Electronics in Agriculture*, *152*, 363–374. https://doi.org/10.1016/j.compag.2018.07.030

Yan, T., Zhu, H., Sun, L., Wang, X., Ling, P. (2019). Investigation of an Experimental Laser Sensor-Guided Spray Control System for Greenhouse Variable-Rate Applications. *Transactions of the ASABE*, *62*(4), 899–911. https://doi.org/10.13031/trans.13366

Zhu, H., Salyani, M., Fox, R.D. (2011) A portable scanning system for evaluation of spray deposit distribution. *Computers and Electronics in Agriculture Volume 76, Issue 1, March 2011, Pages 38-43.* https://doi.org/10.1016/j.compag.2011.01.003

Appendix A

Source code (MATLAB R2019a ver. 9.6.0.1114505, MathWorks, Natick, Massachusetts, USA)

A.1 3-D Map Construction and Filtering

```
% Loading the data from the file saved during the scan run into variables
parameters = load ("C:\laserdata\"+ para_filename+".txt");
Speed = parameters(1,1);
Speed_const=(0.025/720)*(Speed*447.04);
Ground_Level = parameters(2,1)*1000;
Range = (parameters(3,1)*1000);
No_Nozzle = parameters(4,1);
Nozzle_Spacing = parameters(5,1);
Dist_of_first_right_nozzle_from_laser = parameters(6,1);
Dist_of_first_left_nozzle_from_laser = parameters (7,1);

data = load ("C:\laserdata\"+data_filename+".txt");

%First using nameplace x,y,z parameters before the dataset is limited by the set greenhouse
range and ground points have been removed. Nameplace arrays have to be used since we need to
initialize the 'z' parameters before filtering

nameplace_x = data(:,1);
nameplace_y = data(:,2);
nameplace_z=[];
j=1;
for i=1:length(nameplace_x)
    nameplace_z(j) = i*Speed_const;
    j=j+1;
end
```

```
nameplace_z=nameplace_z';

x=[];y=[];z=[];
%Filtering the data based on greenhouse dimensions
for i=1:length(nameplace_x)
   if(nameplace_y(i)>-Range && nameplace_y(i)<Range && nameplace_x(i)>600
&&nameplace_x(i)<(Ground_Level))
       x=[x;nameplace_x(i)];
       y=[y;nameplace_y(i)];
       z=[z;nameplace_z(i)];
   end
end

Raw_Data = [x y z];

%Removing noise from the filtered dataset
ptCloud= pointCloud(Raw_Data);
ptCloudA= pcdenoise(ptCloud);
Raw_Data = ptCloudA.Location(:,:);
```

A.2 Clustering Algorithm

```
% Copying the dataset into a dummy variable so as to not affect the main variable
Dummy_Data=Raw_Data;
no_of_clus=1;
Clusters={};

while (isempty(Dummy_Data)==0)
   Not_in_clus = [];
   Pres_in_clus = [];
   Dummy_Data=sortrows(Dummy_Data,1);
   local_maxima = Dummy_Data(1,:);
```

```
    threshold = linspace (175,10,((Ground_Level+20)-local_maxima(1,1)));
    [nr,nc]=size(Dummy_Data);

    Pres_in_clus = [Pres_in_clus;local_maxima];
    Not_in_clus = [Not_in_clus;40000 40000 40000];

    Idx=rangesearch([Dummy_Data(:,2) Dummy_Data(:,3)],[local_maxima(:,2)
local_maxima(:,3)],750,'SortIndices',true);
    Idx=sort(Idx{1,1});
    length_of_Idx=length(Idx);



    for i=2:length_of_Idx

        distances_to_P = sqrt((Pres_in_clus(:,2)-Dummy_Data(Idx(i),2)).^2 + (Pres_in_clus(:,3)-
Dummy_Data(Idx(i),3)).^2);
        distances_to_N = sqrt((Not_in_clus(:,2)-Dummy_Data(Idx(i),2)).^2 + (Not_in_clus(:,3)-
Dummy_Data(Idx(i),3)).^2);

        if (round(Dummy_Data(Idx(i),1)-local_maxima(1,1))>0)
            indi_threshold = threshold(round(Dummy_Data(Idx(i),1)-local_maxima(1,1)));
        else
            indi_threshold = threshold(1);
        end

        if(min(distances_to_P)<indi_threshold && min(distances_to_P)<=min(distances_to_N))
            Pres_in_clus = [Pres_in_clus;Dummy_Data(Idx(i),:)];
        elseif (min(distances_to_P)<indi_threshold && min(distances_to_P)>min(distances_to_N))
            Not_in_clus = [Not_in_clus;Dummy_Data(Idx(i),:)];
        elseif (min(distances_to_P)>indi_threshold)
            Not_in_clus = [Not_in_clus;Dummy_Data(Idx(i),:)];
```

```
        end

    end

    Dummy_Data = setdiff(Dummy_Data,Pres_in_clus,'rows');
    Clusters{no_of_clus,1}=Pres_in_clus;
    no_of_clus = no_of_clus+1;

end



Clusters = Clusters(cellfun(@(Clusters) length(Clusters)>=60, Clusters)); % Removing clusters that have less than 40 points

Processed_Data=Clusters;
Clus_no=numel(Clusters);

[Mirrored_Data] = Mirroring(Processed_Data,Clus_no,Ground_Level);
```

A.3 Mirroring Algorithm

```
function [Mirrored_Data] = Mirroring(Processed_Data,Clus_no,Ground_Level)
%% Filtering the clusters

Dummy_Data = Processed_Data;
distances_from_centroid=[];
angle_from_centroid=[];

%Removing points that are greater than or lesser than mean+/-2 standard deviations
for k=1:Clus_no
    len=length(Dummy_Data{k,1});
```

```
    centroid_x= mean(Dummy_Data{k,1}(:,1));
    centroid_y= mean(Dummy_Data{k,1}(:,2));
    centroid_z= mean(Dummy_Data{k,1}(:,3));

    for i=1:len
        y_pt= Dummy_Data{k,1}(i,2);
        z_pt= Dummy_Data{k,1}(i,3);
        distances_from_centroid=[distances_from_centroid, (sqrt((y_pt-centroid_y)^2 + (z_pt-
centroid_z)^2))];
        angle_from_centroid=[angle_from_centroid, atan(abs(z_pt-centroid_z)/abs(centroid_y-
y_pt))];
    end

    %Calculating the Mean and Standard Deviation of the distances for each
    %cluster to find outliers
    avg=mean(distances_from_centroid);
    sd=sqrt(var(distances_from_centroid));

    u_lim= avg+(1.96*sd); %Upper limit

    %Replacing all the outliers by Nan (Not a number)
    for j=1:len
        if (Dummy_Data{k,1}(j,2)<centroid_y)
            if (distances_from_centroid(j)>u_lim && angle_from_centroid(j)<((pi/180)*35)) %||
distances_from_centroid(j)<l_lim)
                Dummy_Data{k,1}(j,:)=nan;
            end
        end
    end

    distances_from_centroid=[];
```

```
    angle_from_centroid=[];
end

%Removing the points that are Nan (Not a number)
for k=1:Clus_no
i=1;
    len=length(Dummy_Data{k,1});
    while (i<=len)
        if(isnan(Dummy_Data{k,1}(i,1))==1)
            Dummy_Data{k,1}(i,:)=[];
            len=length(Dummy_Data{k,1});
            i=1;
        else
            i=i+1;
        end

    end

end

%% Mirroring the data

j=0;
Mirrored_Data={};
Nameplace_Matrix=[];
Test_Array =[];
hold on
for k=1:Clus_no
    if (abs(mean(Dummy_Data{k,1}(:,2)))>300) %Mirror only the clusters beyond 300mm from
the sensor
        [R,C,Xb] = ExactMinBoundCircle([Dummy_Data{k,1}(:,2),Dummy_Data{k,1}(:,3)]);
```

```
t = linspace(pi/2,3*pi/2,200); %Using only a semi-circle to find the two points that define the diameter of the bounding circle

bound_cir_y = R*cos(t) + C(1); %Bounding circle center y-coordinate
bound_cir_z = R*sin(t) + C(2); %Bounding circle center z-coordinate

%The points that define the diamter that splits the bounding cicrle
y_upper_lim=bound_cir_y(end);
z_upper_lim=bound_cir_z(end);
y_lower_lim=bound_cir_y(1);
z_lower_lim=bound_cir_z(1);

%Mirroring the points that fall to the right of the splitting
%plane(Diameter of the bounding circle)
for i=1:length(Dummy_Data{k,1})
    y_org=Dummy_Data{k,1}(i,2); z_org= Dummy_Data{k,1}(i,3); x_org=Dummy_Data{k,1}(i,1); %Original data points from the Dummy_Data matrix
    if (abs(y_org)>abs(y_upper_lim))
        continue;
    else
        y_mirrored= 2*(y_upper_lim + ( (((y_org-y_upper_lim)*(y_lower_lim-y_upper_lim))+((z_org-z_upper_lim)*(z_lower_lim-z_upper_lim)))/((y_lower_lim-y_upper_lim)^2+(z_lower_lim-z_upper_lim)^2))*(y_lower_lim-y_upper_lim))-y_org;
        z_mirrored= 2*(z_upper_lim + ( (((y_org-y_upper_lim)*(y_lower_lim-y_upper_lim))+((z_org-z_upper_lim)*(z_lower_lim-z_upper_lim)))/((y_lower_lim-y_upper_lim)^2+(z_lower_lim-z_upper_lim)^2))*(z_lower_lim-z_upper_lim))-z_org;
        Nameplace_Matrix=[Nameplace_Matrix; x_org y_mirrored z_mirrored ; x_org y_org z_org];
    end
end
j=j+1;
```

```
        Mirrored_Data{j,1}= Nameplace_Matrix;
        Nameplace_Matrix=[];
    else
        j=j+1;
        Mirrored_Data{j,1}=Dummy_Data{k,1};

    end
    Test_Array=[];
end

y_conv=[];z_conv=[];
for i=1:Clus_no
    [R,C,Xb] = ExactMinBoundCircle([Mirrored_Data{i,1}(:,2),Mirrored_Data{i,1}(:,3)]);
    t = linspace(0,2*pi,20);

    y_conv = (0.5*R)*cos(t) + C(1);
    z_conv = (0.5*R)*sin(t) + C(2);
    inPoints = polygrid(y_conv,z_conv,0.01);
    x_conv=(Ground_Level).*ones(size(inPoints(:,1)));
    Mirrored_Data{i,1}=[Mirrored_Data{i,1};x_conv inPoints(:,1) inPoints(:,2)];
    y_conv=[];z_conv=[];H=[];
end
end
```

A.4 Overall Processing Algorithm Flowchart

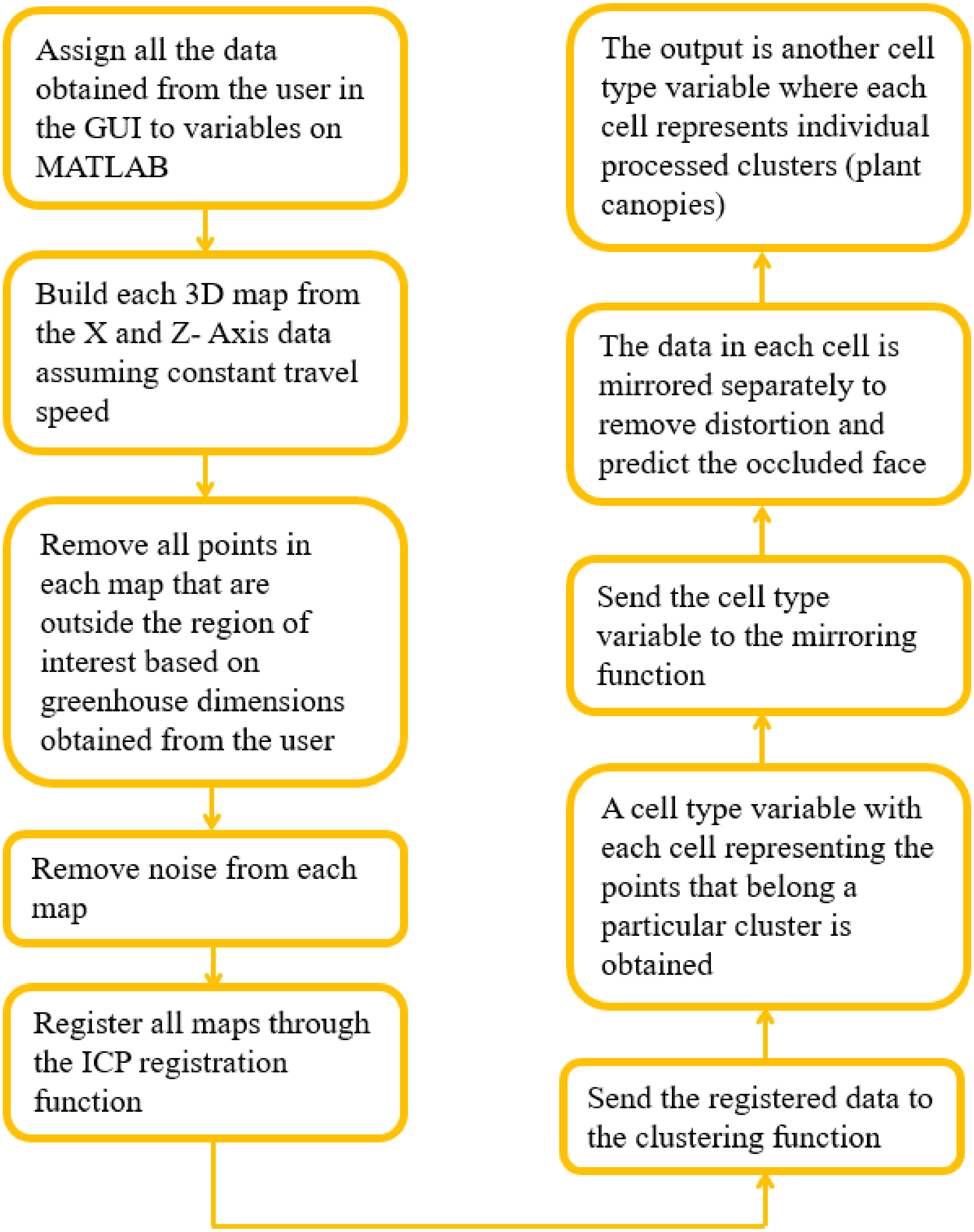
Assign all the data obtained from the user in the GUI to variables on MATLAB
Build each 3D map from the X and Z- Axis data assuming constant travel speed
Remove all points in each map that are outside the region of interest based on greenhouse dimensions obtained from the user
Remove noise from each map
Register all maps through the ICP registration function
Send the registered data to the clustering function
A cell type variable with each cell representing the points that belong a particular cluster is obtained
Send the cell type variable to the mirroring function
The data in each cell is mirrored separately to remove distortion and predict the occluded face
The output is another cell type variable where each cell represents individual processed clusters (plant canopies)

A.5 Spray Rate and Duty Cycle Calculation

```
Vol_per_section={};
Pts_per_section={};
Density_per_section={};
inc=1;

Dum_Mat = cell2mat(Dummy_Mirrored_Data);
length_data=[];
length_data=length(Dummy_Mirrored_Data{1,1});
for i=2:Clus_no
length_data=[length_data;length_data(i-1)+length(Dummy_Mirrored_Data{i,1})];
end
Valid_Indices_Track={};
cluster_x=[];cluster_y=[];cluster_z=[];
valid_x=[];valid_y=[];valid_z=[];
cluster_indices=[];
valid_indices=[];

length_dataset=max(Dum_Mat(:,3))-min(Dum_Mat(:,3));
Segment_length= 721*5*Speed_const; %The nozzles are triggered every 0.125s which is
equivalent to 5 scan lines
travel_limit = round(length_dataset/Segment_length);

low_limit = min(Dum_Mat(:,3))/Speed_const;
Current_Segment_Val=((low_limit)-rem((low_limit),721))*Speed_const;


Slice_length = Nozzle_Spacing; %Assuming there are 10 nozzles

% Initializing a kd-tree searcher to improve speed
```

```
Mdl = KDTreeSearcher([Dum_Mat(:,2) Dum_Mat(:,3)],'BucketSize',20000);
for i=1:travel_limit

    Current_Slice_Val=-(Dist_of_first_right_nozzle_from_laser + (Nozzle_Spacing/2));
    for j=1:No_Nozzle

        Idx = rangesearch(Mdl,[Current_Slice_Val
Current_Segment_Val],750);%Distance','euclidean');%,'Scale',iqr([Dum_Mat(:,2)
Dum_Mat(:,3)]));

        if (length(Idx{1,1})>3)
            Idx=cell2mat(Idx);
           % Finding the valid indexes that lie in the particular segment
           % and slice
            for k=1:length(Idx)
                if (Dum_Mat(Idx(k),3)>=Current_Segment_Val &&
Dum_Mat(Idx(k),3)<=(Current_Segment_Val+Segment_length) &&
Dum_Mat(Idx(k),2)>=Current_Slice_Val && Dum_Mat(Idx(k),2)<=(Current_Slice_Val +
Slice_length))
                    valid_x=[valid_x;Dum_Mat(Idx(k),1)];
                    valid_y=[valid_y;Dum_Mat(Idx(k),2)];
                    valid_z=[valid_z;Dum_Mat(Idx(k),3)];
                    valid_indices = [valid_indices;Idx(k)];
                end
            end
            valid_data=[valid_x valid_y valid_z];
            valid_x=[];valid_y=[];valid_z=[];
          %Finding the index that belong to a particular cluster
          while (isempty(valid_data)==0)
            for l=1:length(length_data)
```

```
    if(min(valid_indices)<=length_data(l))
        break;
    end
end

%Assigning values to the valid points that belong to a cluster
for m=1:length(valid_indices)
    if(valid_indices(m)<=length_data(l))
        cluster_x=[cluster_x;Dum_Mat(valid_indices(m),1)];
        cluster_y=[cluster_y;Dum_Mat(valid_indices(m),2)];
        cluster_z=[cluster_z;Dum_Mat(valid_indices(m),3)];
        cluster_indices=[cluster_indices;valid_indices(m)];
    end
end

cluster_data = [cluster_x cluster_y cluster_z];
cluster_x=[];cluster_y=[];cluster_z=[];



Pts_per_section{i,j}{1,inc}=cluster_data;
shp=alphaShape(Pts_per_section{i,j}{1,inc},inf);
Vol_per_section{i,j}{1,inc} = volume(shp);
width_of_dataset=(max(cluster_data(:,2))-min(cluster_data(:,2)));
length_of_dataset=(max(cluster_data(:,3))-min(cluster_data(:,3)));
height_of_dataset=(max(cluster_data(:,1))-min(cluster_data(:,1)));
if (Vol_per_section{i,j}{1,inc}>0)
    Density_per_section{i,j}{1,inc} =
Vol_per_section{i,j}{1,inc}/(width_of_dataset*length_of_dataset*height_of_dataset);
else
    Density_per_section{i,j}{1,inc} = 0;
end
```

```
            valid_data = setdiff(valid_data,cluster_data,'rows');
            valid_indices = setdiff(valid_indices, cluster_indices);
            inc=inc+1;
          end

        end

        Current_Slice_Val=Current_Slice_Val - Slice_length;
        inc=1;
    end

    Current_Segment_Val = Current_Segment_Val + Segment_length;
    inc=1;
end
toc
%%

[i_length,j_length]=size(Vol_per_section);
Max_Height=[];
density=[];
Right_DC=zeros([travel_limit,No_Nozzle*2]);
Right_DC_Hex{15,No_Nozzle*2}={'0'};
Right_Spray_Rate = zeros([travel_limit,No_Nozzle]);
Segment_Height = zeros([travel_limit,No_Nozzle]);


for i=1:i_length
    for j=1:j_length
        Sum_Vol =0;
        Max_Density_of_section=0;
        for k=1:length(Vol_per_section{i,j})
```

```
            Sum_Vol = Sum_Vol + Vol_per_section{i,j}{1,k};
            Max_Density_of_section=
max(Max_Density_of_section,Density_per_section{i,j}{1,k});
            if (isempty(Pts_per_section{i,j})==0)
               Max_Height=[Max_Height,min(Pts_per_section{i,j}{1,k}(:,1))];

            else
               Max_Height=G_Level-1;
            end
        end
        Seg_Height=min(Max_Height);

        if (isempty(Seg_Height)==1)
            Seg_Height=G_Level-1;
        end
        density(i,j) = Max_Density_of_section;
        Segment_Height(i,j) = Seg_Height;
        Right_Spray_Rate(i,j) = ((60*(Slice_length/1000)*((Ground_Level-
Seg_Height)/1000)*(Speed*0.44704)*density(i,j)*0.13)/0.675)*100;
        if (Right_Spray_Rate(i,j)==0)
            Right_DC(i,j)=0;
        elseif(round(Right_Spray_Rate(i,j))<20)
            Right_DC(i,j)=20;
        elseif(round(Right_Spray_Rate(i,j))>99)
            Right_DC(i,j)=99;
        else
            Right_DC(i,j) = round(Right_Spray_Rate(i,j));
        end
        Max_Height=[];
    end
end
```

```
Right_DC=flip(Right_DC,2);
[nr,nc]=size(Right_DC);
clear R_DC_Hex;
R_DC_Hex{15,1}={};
for i=1:nr
    k=i;
    R_DC_Hex{k,1}= "ff";
    for j=1:nc
        Right_DC_Hex{k,j}=num2str(Right_DC(i,j));
        if round(Right_DC(i,j))<10
            Right_DC_Hex{k,j}="0"+Right_DC_Hex{k,j};
        end
        R_DC_Hex{k,1} = strcat(R_DC_Hex{k,1},Right_DC_Hex{k,j});
    end
    R_DC_Hex{k,1}= R_DC_Hex{k,1} + "55";
end
R_DC_Hex{k+1,1}= "ff000000000000000000000000000000000000000055";


 %% Left Nozzles
% Clearing variables used during right nozzle spray rate calculations
tic
Vol_per_section={};
Pts_per_section={};
Density_per_section={};
inc=1;

cluster_x=[];cluster_y=[];cluster_z=[];
valid_x=[];valid_y=[];valid_z=[];
```

```
cluster_indices=[];
valid_indices=[];

low_limit = min(Dum_Mat(:,3))/Speed_const;
Current_Segment_Val=((low_limit)-rem((low_limit),721))*Speed_const;



for i=1:travel_limit
    Current_Slice_Val=Dist_of_first_left_nozzle_from_laser + (Nozzle_Spacing/2);
    for j=1:No_Nozzle

  % Initializing a kd-tree searcher to improve speed

        Idx = rangesearch(Mdl,[Current_Slice_Val
Current_Segment_Val],750);%Distance','euclidean');%,'Scale',iqr([Dum_Mat(:,2)
Dum_Mat(:,3)]));

        if (length(Idx{1,1})>3)
%             Idx=sort(Idx{1,1});
                Idx=cell2mat(Idx);
              % Finding the valid indexes that lie in the particular semnet
              % and slice
                for k=1:length(Idx)
                    if (Dum_Mat(Idx(k),3)>=Current_Segment_Val &&
Dum_Mat(Idx(k),3)<=(Current_Segment_Val+Segment_length) &&
Dum_Mat(Idx(k),2)<=Current_Slice_Val && Dum_Mat(Idx(k),2)>=(Current_Slice_Val -
Slice_length))
                        valid_x=[valid_x;Dum_Mat(Idx(k),1)];
                        valid_y=[valid_y;Dum_Mat(Idx(k),2)];
                        valid_z=[valid_z;Dum_Mat(Idx(k),3)];
                        valid_indices = [valid_indices;Idx(k)];
```

```
        end
    end
    valid_data=[valid_x valid_y valid_z];
    valid_x=[];valid_y=[];valid_z=[];
%Finding the index that belong to a particular cluster
while (isempty(valid_data)==0)
    for l=1:length(length_data)
        if(min(valid_indices)<=length_data(l))
            break;
        end
    end

    %Assigning values to the valid points that belong to a cluster
    for m=1:length(valid_indices)
        if(valid_indices(m)<=length_data(l))
            cluster_x=[cluster_x;Dum_Mat(valid_indices(m),1)];
            cluster_y=[cluster_y;Dum_Mat(valid_indices(m),2)];
            cluster_z=[cluster_z;Dum_Mat(valid_indices(m),3)];
            cluster_indices=[cluster_indices;valid_indices(m)];
        end
    end

    cluster_data = [cluster_x cluster_y cluster_z];
    cluster_x=[];cluster_y=[];cluster_z=[];

    Pts_per_section{i,j}{1,inc}=cluster_data;
    shp=alphaShape(Pts_per_section{i,j}{1,inc},inf);
    Vol_per_section{i,j}{1,inc} = volume(shp);
    width_of_dataset=(max(cluster_data(:,2))-min(cluster_data(:,2)));
    length_of_dataset=(max(cluster_data(:,3))-min(cluster_data(:,3)));
    height_of_dataset=(max(cluster_data(:,1))-min(cluster_data(:,1)));
```

```
            if (Vol_per_section{i,j}{1,inc}>0)
                Density_per_section{i,j}{1,inc} =
Vol_per_section{i,j}{1,inc}/(width_of_dataset*length_of_dataset*height_of_dataset);
            else
                Density_per_section{i,j}{1,inc} = 0;
            end
            valid_data = setdiff(valid_data,cluster_data,'rows');
            valid_indices = setdiff(valid_indices, cluster_indices);
            inc=inc+1;
        end

    end
    Current_Slice_Val=Current_Slice_Val + Slice_length;
    inc=1;
  end
  Current_Segment_Val = Current_Segment_Val + Segment_length;
  inc=1;
end

%%

[i_length,j_length]=size(Vol_per_section);
Max_Height=[];
density_left=[];
Left_DC=zeros([travel_limit,No_Nozzle]);
% Left_DC_Hex{travel_limit,No_Nozzle}={'0'};
Left_DC_Hex{15,No_Nozzle}={'0'};
Left_Spray_Rate = zeros([travel_limit,No_Nozzle]);

for i=1:i_length
  for j=1:j_length
```

```
        Sum_Vol =0;
        Max_Density_of_section=0;
        for k=1:length(Vol_per_section{i,j})
            Sum_Vol = Sum_Vol + Vol_per_section{i,j}{1,k};
            Max_Density_of_section=
max(Max_Density_of_section,Density_per_section{i,j}{1,k});
            if (isempty(Pts_per_section{i,j})==0)
                Max_Height=[Max_Height,min(Pts_per_section{i,j}{1,k}(:,1))];
            else
                Max_Height=G_Level-1;
            end
        end
        Seg_Height=min(Max_Height);
        if (isempty(Seg_Height)==1)
            Seg_Height=G_Level-1;
        end
        density_left(i,j)=Max_Density_of_section;
        Left_Spray_Rate(i,j) = ((60*(Slice_length/1000)*((Ground_Level-
Seg_Height)/1000)*(Speed*0.44704)*density_left(i,j)*0.13)/0.675)*100;

        if (Left_Spray_Rate(i,j)==0)
            Left_DC(i,j)=0;
        elseif(round(Left_Spray_Rate(i,j))<20)
            Left_DC(i,j)=20;
        elseif(round(Left_Spray_Rate(i,j))>99)
            Left_DC(i,j)=99;
        else
            Left_DC(i,j) = round(Left_Spray_Rate(i,j));
        end
        Max_Height=[];
    end
```

```
end



[nr,nc]=size(Left_DC);
L_DC_Hex{nr,1}={};
for i=1:nr
    L_DC_Hex{i,1}= "ff";
    for j=1:nc
        Left_DC_Hex{i,j}=num2str(Left_DC(i,j));
        if round(Left_DC(i,j))<10
            Left_DC_Hex{i,j}="0"+Left_DC_Hex{i,j};
        end
            L_DC_Hex{i,1} = strcat(L_DC_Hex{i,1},Left_DC_Hex{i,j});
    end
    L_DC_Hex{i,1}= L_DC_Hex{i,1} + "0000000000000000000055";
end

L_DC_Hex{i+1,1}= "ff000000000000000000000000000000000000000055";
toc
%%
```

Appendix B

B.1 User's Guide to Operate the Intelligent Sprayer

- Connect the laser sensor to the computer through the ethernet cable
- Connect the computer to the PWM Controller through the COM ports – COM1 for the right spray boom and COM2 for the left spray boom
- Measure the distance from the laser sensor to end of the greenhouse bay (half of the total width since the laser is mounted onto the center of the spray boom)
- Measure the nozzle spacing
- Count the number of nozzles on the boom
- Measure the distance of the first nozzles on the right and left spray boom to the laser sensor.
- Measure the distance between the laser sensor and the nozzles
- Set the speed of the boom (Values range from 1-16 which referred to speeds from 0.044704 m/s to 0.40234 m/s)

First Step is the Scan Run:

- Open the Sprayer Program on the computer
- Fill in the measured parameters in the 'Data Collection' Tab
- Click the 'Play' icon button and wait for the message bar at the bottom to say "Recording Data…"
- Move the spray boom across the plant canopies at the previously fixed speed
- Click the 'Stop' button when all the plant canopies have been scanned
- Wait for the message "Recording has Stopped"

- Minimize the Spray Program

Second Step to identify the spray rates

- Run the CHBC processing program on MATLAB and enter the file name of the saved data from the scan run. (Saved in a specific location on the computer).
- This will result in two new files being recorded- The duty cycle sequence for the right boom, the duty cycle sequence for the left boom)

Third Step is the Spray Run

- Minimize the MATLAB program and open the ‘Spray Application’ tab on the Sprayer Program
- Enter the parameter required
- Test the nozzles if required by setting a duty cycle on the sliding bar and clicking the ‘Test Nozzles’ button
- Move the spray boom back to its initial position
- Click the ‘Play’ icon button and move the spray boom at the same speed setting as in the scan run
- Wait for the message “Looking for canopies…”
- Once the laser passes the first set of canopies, the message “Canopies Detected!” will be printed
- The duty cycle sequence will then be triggered based on the distance between the nozzles and the sensor and the speed
- The system will apply a variable-rate spray over the length of the travel distance

B.2 Spray Run Operational Flowchart